

**WL-TR-96-3118**



**PROPAGATION CHARACTERISTICS  
AND THERMAL PERFORMANCE OF  
SOLID PARTICULATE AEROSOLS**

**A. E. S. GREEN**

**University of Florida  
Clean Combustion Technology Laboratory  
Gainesville FL 32611-2050**

**DTIC QUALITY INSPECTED 4**

**SEPTEMBER 1995**

**FINAL REPORT FOR JULY 1994--FEBRUARY 1995**

**Approved for public release; distribution unlimited**

**FLIGHT DYNAMICS DIRECTORATE  
WRIGHT LABORATORY  
AIR BASE TECHNOLOGY BRANCH  
TYNDALL AFB FL 32403-5323**

**19961016 109**

## NOTICES

WHEN GOVERNMENT DRAWINGS, SPECIFICATIONS, OR OTHER DATA ARE USED FOR ANY PURPOSE OTHER THAN IN CONNECTION WITH A DEFINITE GOVERNMENT-RELATED PROCUREMENT, THE UNITED STATES GOVERNMENT INCURS NO RESPONSIBILITY OR ANY OBLIGATION WHATSOEVER. THE FACT THAT THE GOVERNMENT MAY HAVE FORMULATED OR IN ANY WAY SUPPLIED THE SAID DRAWINGS, SPECIFICATIONS, OR OTHER DATA, IS NOT TO BE REGARDED BY IMPLICATION, OR OTHERWISE IN ANY MANNER CONSTRUED, AS LICENSING THE HOLDER, OR ANY OTHER PERSON OR CORPORATION; OR AS CONVEYING ANY RIGHTS OR PERMISSION TO MANUFACTURE, USE, OR SELL ANY PATENTED INVENTION THAT MAY IN ANY WAY BE RELATED THERETO.


The Public Affairs Office (PA) has reviewed this report and it is releasable to the National Technical Information Service (NTIS). At NTIS, the report will be made available to the general public, including foreign nationals.

This technical report has been reviewed and is approved for publication.




ROBERT A. TETLA  
Project Officer

FOR THE COMMANDER:



RICHARD N. VICKERS  
Chief, Infrastructure Technology Section



EDGAR F. ALEXANDER  
Chief, Air Base Technology Branch

If your address has changed, if you wish to be removed from our mailing list, or if the addressee is no longer employed by your organization, please notify WL/FIVC, Tyndall AFB Florida 32403-5323, to help maintain a current mailing list.

Copies of this report should not be returned unless required by security considerations contractual obligations, or notice on a specific document.



## TABLE OF CONTENTS

<u>Section</u>	<u>Title</u>	<u>Page</u>
I	INTRODUCTION .....	1
	A. OBJECTIVE .....	1
	B. BACKGROUND .....	2
	C. FIRE SUPPRESSION MECHANISMS .....	3
II	FLAME SUPPRESSION AND HEAT ABSORPTION STUDIES. ....	5
	A. PRIOR PYROTECHNICALLY GENERATED SUPPRESSANT WORK ..	5
	B. CHARACTERISTICS OF SFEs. ....	7
	C. SINGLE CHANNEL STUDIES. ....	8
	1. Cylinder and Piston .....	8
	2. Bell Jar .....	10
	3. Syringe Apparatus .....	10
	D. OVERVIEW OF MULTIPLE CHANNEL DEVICES .....	11
	1. (MWCD) SFE .....	11
	2. (MFTB) SFE .....	11
	3. (CHRD) SFE .....	11
	4. (RCBD) SFE .....	11
III	WET CERAMIC DEVICES .....	12
	A. THE JANUARY 12, 1995 DEVICE .....	12
	B. MATERIALS FOR MULTICHANNEL DEVICES (MMCD) .....	14
	1. Clay Extrusions .....	14
	2. Fiberfrax .....	14
	3. Woven Fiberfrax .....	14
	4. Fiberfrax Paper. ....	15
	5. Coated Wire Screen .....	15
	6. Clay Plug .....	15
	7. Porous Metallic Fins .....	15
	8. Stabilized Water .....	15
	9. Water Sealants .....	15
	10. Metal - Ceramic Composites .....	15
	C. CERAMIC CHANNEL STUDY - HEAT TRANSFER ANALYSIS .....	16
	1. Introduction .....	16
	2. Symbols .....	16
	3. Modeling the Ceramic Channel .....	16
	4. Testing the Model .....	17
	a. Multichannel Device. ....	17
	b. Bunsen Experiments .....	19
	5. Optimizing Ceramic Channel Configurations .....	20



# TABLE OF CONTENTS

## (Concluded)

<u>Section</u>	<u>Title</u>	<u>Page</u>
IV	MULTICHANNEL FIRE TUBE BOILER .....	23
	A. AUTOMOTIVE HEAT EXCHANGERS .....	23
	B. HEAT TRANSFER ANALYSIS IN A FIRE TUBE BOILER DEVICE ...	24
	1. Introduction	
	2. Modeling the Fire Tube	
	3. Experimentation	
V	HEAT RETENTION AND RADIATIVE DEVICES ... ..	27
	A. CARBONATE HEAT RETENTION DEVICES (CHRD) .....	27
	B. RADIATIVE COOLED AND BAFFLED DEVICE (RCBD) .....	29
	C. THROWABILITY OF SFE DEVICES .....	29
VI	MECHANISMS OF FLAME SUPPRESSION .....	31
	A. FUNDAMENTALS .....	31
	B. PROPANE FLAME - SUPPRESSANT INTERACTIONS .....	33
	C. STRAY LIGHT REJECTION .....	35
	D. SUPPRESSION OF PAN FIRES .....	37
	E. METHANE - 1301 SPECTRA .....	38
	G. KINETIC MODELING OF METHANE FLAME SPECTRA .....	40
VII	DISCUSSION AND CONCLUSIONS .....	47
	A. FLAME SUPPRESSION .....	47
	1. The Understanding of Flame Suppression .. ..	47
	2. Radiation - FR - Coupling. ....	47
	3. Hydrogen - 1301 Flames. ....	48
	4. Benign Sources of Fine Aerosols	49
	B. DESIGN AND CONSTRUCTION OF HAND THROWN SFE CANISTERS .	50
	C. POTENTIAL OFFSHOOTS OF PROGRAM .....	51
	1. Stationary Passive Flooding Devices .....	51
	2. Hand Held Fire Extinguishers .....	51
	3. Fire Diagnostics .....	51
	4. RFRSC Hypothesis. ....	51
	D. CONCLUSIONS	53
	E. ACKNOWLEDGEMENTS .....	55
VIII	REFERENCES .....	56

## LIST OF FIGURES

<u>Figure</u>	<u>Title</u>	<u>Page</u>
1	Experimental arrangement for spectroscopic analysis of pool flame with aerosol suppressant .....	4
2	Heptane and aerosol suppressant. (A) no suppressant, (B) aerosol added .....	4
3	Modified Wien's displacement law estimate of SFE combustion temperature .....	9
4	Final piston - cylinder device .....	9
5	Schematic diagram of the multichannel wet ceramic device (MWCD) .....	13
6	Theoretical performance curves form MWCD model .....	19
7	Thermocouple data from Bunsen experiment. ....	21
8	Theoretical performance curve for Bunsen model .....	21
9	Schematic diagram of a fire tube. ....	26
10	Theoretical performance curves for 'optimal' fire tube devices. ....	26
11	Radiative cooled and baffled device (RCBD) .....	30
12	Methanol pool fire with halon 1211 suppressant : (a) no suppressant, (b) 1211 at 26 ml/min, (c) 1211 at 40 ml/min, (d) 1211 at 60 ml/min, (e) 1211 at 128 ml/min. ....	34
13	Methanol pool fire with halon 1211 suppressant (OH region). Notice the reversal of trend; (a) no suppressant, (b) 1211 at 26 ml/min, (c) 1211 at 40 ml/min, (d) 1211 at 60 ml/min, (e) 1211 at 128 ml/min .....	34
14	(A) MUV spectra of a propane diffusion flame with halon 1211 added to the fuel stream. (B) similar case with good stray-light-rejection measures with tentative identification of molecular features .....	36
15	Premixed methane-air flame spectrum taken with 400 1/mm grating (A) without halon, (B) with halon. ....	39
16	Premixed methane-air flame spectrum taken with 2400 1/mm grating (A) without halon (B) with halon .....	39

17	Diffusion flame spectrum (A) without solar blind filter (counts divided by 4) (B) with solar blind filter (C) with solar blind filter and halon .....	41
18	Voltage output of thermopile vs. halon injection rate .....	41
19	Kinetic model results for premixed methane flame with assumed temperature-time profile (A) major species, (B) free radicals and minor species, (C) major species when halon 1301 is injected, (D) free radicals and minor species when halon 1301 is injected (note changes in vertical scales) .....	43
20	Multichannel fire-tube boiler (MFTB) .....	52
21	Hand fire extinguisher exterior cooling .....	52
22	Illustration of a possible cylindrical radiation device. ....	54

## LIST OF TABLES

<u>Table</u>	<u>Title</u>	<u>Page</u>
1	Heating Values of SFE as Measured with a Parr Calorimeter (in BTU/lb) .....	6
2	Thermal Properties of Common Materials .....	6
3	Dissociation Temperatures of Ceramic Materials Adapted from Ceramic Glazes by C.W. Parmelee, Industrial Publications, Inc., Chicago, IL 1951 .....	6
4	Heat Absorption by Selected Materials .....	28
5	Experimental Results Using Dolomite Blends .....	28
6	Reactions in Hydrogen Flame Leading to Hydroxyl Radicals ...	46
7	Reactions in Methane Flames Leading to Hydroxyl Radicals. ...	46



## PREFACE

This report was prepared by Alex E. S. Green, Principle Investigator. Dr Green is a Graduate Research Professor of Mechanical Engineering and Nuclear Engineering Sciences in the College of Engineering and Director of the Clean Combustion Technology Laboratory (CCTL) and the Interdisciplinary Center for Aeronomy and Other Atmospheric Sciences (ICAAS). Major contribution to Sections III and IV were made by James Mullin, partly in connection with his M.S. degree program in Mechanical Engineering. Important contributions to Section VI were made by Hui Xue, partly in connection with his M.S. degree program in Electrical Engineering. The work of Dale Walter, who completed his M.S. degree program in Mechanical Engineering in December 1994 is also reflected in this report. Other scientific and technical participants in this overall study include Mr Donald Denniston, Drs. Theresa Miller and Juan Vitali, Cameron Harper, Charles Kibert Jr. and Douglas Tarbox. Manuscripts of the interim report of February 24, 1995 and this final report, were prepared by Freda K. Green. The work was conducted at the facilities of the Clean Combustion Technology Laboratory in the Space Sciences Research Building of the University of Florida.

This document is the final report on a contract between the Fire Testing and Research Center (FTRC) at the University of Florida, the Applied Research Associates (ARA), Inc., P.O. Box 40128, Tyndall Air Force Base, Florida 32403, and the Air Base Fire Protection and Crash Rescue Systems Branch of Wright Laboratories (WL/FIVCF), Tyndall Air Force Base, Florida, 32403, under ARA Contract S-5000.18. (Task 3.08) "Propagation Characteristics of Solid Particulate Aerosols". It also includes related work initiated under the subcontract No. S-5000.8 (Task3.06) "Thermal Performance of Solid Particulate Aerosols" initiated in February 1994 and some closely related fundamental investigations supported by the College of Engineering.

The ARA Project Officer is Michael A. Rochefort, the WL/FIVCF Project Officer is Capt. Robert A. Tetla. The Project Director is Dr. Weilin P. Chang, Director of the Center for Fire Testing and Research at the University of Florida.



## EXECUTIVE SUMMARY

### A. OBJECTIVE

The aims of this program are to clarify the mechanism of flame suppression by pyrotechnically generated aerosols, particularly the aerosols generated by Spectrex Fire Extinguishments (SFE) A, B, and C manufactured by the Spectrex Inc. Using this understanding the next objective was to design a hand thrown canister incorporating 500 grams of the pyrotechnique material. The final objective ( optional until funds were made available in January 1995) was to construct throwable devices and to test these devices.

This document is the final report on technical worked performed under ARA Contract S-5000.18. (Task 3.08) "Propagation Characteristics of Solid Particulate Aerosols". It also includes closely related work under the subcontract No. S-5000.8 (Task3.06) "Thermal Performance of Solid Particulate Aerosols" initiated at U.F. in February 1994 and some closely related work on fire suppression mechanisms supported by the College of Engineering of the University of Florida .

The final (July 20, 1994) work plan for Task 3.08 included four sub-tasks

Sub-task 1. Development of a Detailed Plan of Activities

Sub-task 2. Flame Suppression

Sub-task 3. Design of a Hand Thrown EMAA canister

Sub-task 4: (Optional) Construction/Testing of Hand Trown EMAA Canister  
( Incremental funds for this task became available on January 1, 1995.)

The objective of sub-task 2 was to improve our understanding of physical and chemical mechanisms of fire suppression by aerosols. In this connection we have also conducted some laboratory spectroscopic and radiation studies with College of Engineering resources. These were supplementary to the efforts undertaken with resources provided by ARA Contracts S-5000.18. (Task 3.08) and S-5000.8 (Task 3.06).

The objective of sub-task 3 was to conduct studies leading to the design of hand-thrown devices using 500 grams of the Encapsulated Micron Aerosol Agents (EMAA) provided by Spectrex. These pyrotechnical generators burn rapidly, releasing approximately 2200 BTU/lb at temperatures in excess of 3500 °F. The throwable EMAA container was to provide means of reducing the exiting aerosols to below 500 °F. The specific tablets studied have been provided by Spectrex Inc. and are designated SFE-A, B and C. Powders of SFE A and B were also made available.

The objective of sub-task 4 was to construct and test hand-thrown EMAA devices based upon the design consideration reached in sub-task 3.



## B. BACKGROUND

The search for replacements and alternatives for the halon family of chemical fire suppressants has coincided with the development of novel materials and techniques that provide new options for fire protection. Originating as solid materials, micron-size aerosol particles are generated via combustion of a combination of active compound, oxidizer and binder. The Encapsulated Micron Aerosol Agents (EMAA) class of aerosol has been proposed as having superior volumetric efficiency, low initial and life cycle costs, low toxicity and no known global atmospheric environmental impacts such as greenhouse warming and ozone depletion, both of which are problems with halons.

Initial tests by Spectrex and New Mexico Engineering Research Institute (NMERI) and National Institute of Science and Technology (NIST), had indicated that EMMA has potential as a replacement of halons both in fire suppression and inertion environments. Under ARA Subcontract S-5000.8 SETA Task 3.06, "Thermal Performance of Solid Particle Aerosols" we initiated measurements of the thermal output of SFE materials, of potential cooling mechanisms and fire extinguishment processes. We also began exploratory investigations of potential methods of packaging arrangements leading to practical devices.

## C. CONCLUSION

In relation to TASK 3.08 - sub task 2, "Flame Suppression" we have observed correlation between increases in total radiation and decreases in OH emissions suggestive of a physiochemical coupling between the two observables. We use the acronym RFRSC for "radiation- free radical scavenging- coupling" to denote this hypothesis. The specific links we invoked to couple the two observables are supported by a vast body of data in the literatures on the kinetics of combustion, on soot formation and on toxic emissions from the combustion of chlorinated hydrocarbons. Our RFRSC mechanism serves as a natural bridge between the strictly thermal hypothesis of Ewing et. al. and the free radical scavenging hypothesis of Westbrook and should help lead to a unified theory of fire suppression.

Subtasks 3 and 4 of Task 3.08, the design and construction of hand thrown devices charged with 500 grams of SFE consumed most of our efforts through February 1995. By then we had examined and experimentally explored a large number of potential types of devices. We arrived at four major possible design paths and brought a multichannel wet ceramic device close to our estimate of the best physical realization based upon a 500 gram SFE charge. It had a (device/charge) weight ratio of about 6, contained the flame and produced a steam-aerosol exhaust below the ignition point of class A and B materials. A second path, the cylindrical radiator, also looked promising. Subsequently we devoted most of our efforts on Subtasks 3 and 4 to single channel tests and mathematical modeling. Our object was to find more efficient heat absorption techniques leading to a cooler exhaust and a lighter device.

If one is confined to SFE charges it would be prudent, in further R&D, to focus on stationary type devices or single channel fire extinguishers. Successful experience with pyrotechnically generated aerosols in simple devices could be used to address the more difficult problem of designing and constructing hand thrown devices.

## SECTION 1

### INTRODUCTION

#### A. OBJECTIVE

The first objective of this program (sub-task 2) was to clarify the mechanism of flame suppression by pyrotechnically generated aerosols, particularly the aerosols generated by Spectrex Fire Extinguishments (SFE) A, B, and C manufactured by Spectrex Inc. Using this understanding the next objective (sub-task 3) was to design a hand thrown canister incorporating 500 gr of the pyrotechnique material. The final objective (sub-task 4, optional until funds were made available in January 1995) was to construct hand thrown devices and to test these devices.

This document is the final report on technical work performed under ARA Contract S-5000.18. (Task 3.08) "Propagation Characteristics of Solid Particulate Aerosols". It also includes closely related work under the subcontract No. S-5000.8 (Task3.06) "Thermal Performance of Solid Particulate Aerosols" initiated at U.F. in February 1994 and closely related work on fire suppression mechanisms supported by the University of Florida College of Engineering resources.

The July 20, 1994 work plan for Task 3.08 consisted of four sub-tasks

Sub-task 1. Development of a Detailed Plan of Activities

Sub-task 2. Flame Suppression

- 2.1 Prior Related Work
- 2.2 Fundamental Mechanisms
- 2.3 Characteristics of SFEs
- 2.4 Radiative Properties of SFE-Pan Fire Interactions

Sub-task 3. Design of a Hand Thrown EMAA canister

- 3.1 Phosphate Slime Grenades
- 3.2 Cooling EMAA Devices
- 3.3 Suppression of Small Pan Fires with 20 gr Devices
- 3.4 Testing of 100- 200 gr EMAA Devices
- 3.5 Assembly of EMAA Designs and Tests by other groups

Sub-task 4: (Optional) Construction/Testing of Hand Trown EMAA Canister  
( Incremental funds for this option became available on January 1, 1995)

In relation to sub-task 2, to improved our understanding of physical and chemical mechanisms of fire suppression by aerosols we have also conducted some laboratory spectroscopic and radiation studies with College of Engineering resources. These were supplementary to the efforts undertaken with resources provided by ARA Contracts S-5000.18. (Task 3.08) and S-5000.8 (Task3.06).

The objective of sub-task 3 was to conduct studies leading to the design of hand-thrown devices using the Encapsulated Micron Aerosol Agents (EMAA) provided by Spectrex Inc. These pyrotechnical generators burn rapidly, releasing

approximately 2200 BTU/lb at temperatures in excess of 3500 °F. The throwable EMAA container was to provide means of reducing the exiting aerosol to below 500 °F.

The objective of sub-task 4 was to construct and test hand-thrown EMAA devices based upon the design consideration reached in sub-task 3

## B. BACKGROUND

The search for replacements and alternatives for the halon family of chemical fire suppressants has coincided with the development of novel materials and techniques that provide new options for fire protection. Originating as solid materials, micron-size aerosol particles are generated via combustion of a combination of active compound, oxidizer and binder. The Encapsulated Micron Aerosol Agents (EMAA) class of aerosol has been proposed as having superior volumetric efficiency, low initial and life cycle costs, low toxicity and no known global atmospheric environmental impacts such as greenhouse warming and ozone depletion, both of which are problems with halons.

EMAA is a dispersion aerosol that is intended for delivery to the protected area via the combustion of the solid tablet. The dynamics of aerosols are important considerations for two reasons. First, the ability of the particles to remain suspended is obviously connected to the particle size. Second, the aerosol, if it is to replace gases in certain applications, must be able to flow around obstacles. The ability of the aerosol to remain suspended is governed by Stoke's Law which predicts the terminal velocity of the particle through air and consequently the residence time of the aerosol. Micron and submicron particles have a terminal velocity in the order of 0.5 cm/hr or less. The specific tablets studied have been provided by Spectrex and are designated SFE-A, B and C. Powdered forms of SFE A and B were also provided.

Initial testing done by Spectrex and New Mexico Engineering Research Institute (NMERI) and National Institute of Science and Technology (NIST), has indicated that EMAA has potential as a replacement of halons both in fire suppression and inertion environments. Under ARA Subcontract S-5000.8 SETA Subtask 3.06, "Thermal Performance of Solid Particle Aerosols" we initiated in February 1994 measurements of the thermal output of SFE materials, of potential cooling mechanisms and fire extinguishment processes. We also began exploratory investigations of potential methods of packaging arrangements intended to lead to practical devices.

This program was intended to test the propagation capabilities and performance of EMAA, in relationship to the tasks on ARA subcontract No. S-5000.18, "Propagation Characteristics of Solid Particulate Aerosols," (Task 3.08).

The Montreal Protocol and the Clean Air Act of 1990 call for the phase out of halons to protect the stratospheric ozone layer and to avoid greenhouse warming. Pyrotechnically Generated Aerosols (PGA) or Pyrotechnically Generated Gas (PGG) [together to be referred to as Pyrotechnically Generated Suppressants (PGS)] are possible alternatives. Unfortunately the heat and flame connected with their generation might initiate a fire rather than suppress it. By using pyrotechnically generated aerosols or gases we are basically attempting to extinguish fires with fire. Since FIRE, despite its use by mankind for 500 millenia still has many mysteries this is intrinsically a very difficult problem. The fact that the anti-fire, in this case is an

offshoot of rocket propellant technology, is much hotter than the fires to be extinguished multiplies the difficulty. In our sub-task 4 efforts to develop a hand thrown PGA device weight, size and shock resistance requirements further complicated the design and fabrication problem.

### C. FIRE SUPPRESSION MECHANISMS

The search for halon replacements has focused attention on the still unsettled issue of flame extinction mechanisms. A recent article in Chemical and Engineering News (C&EN) [1] describes European quests for halon alternatives. Several points brought out in this article when taken together with general knowledge are particularly relevant to PGS programs. 1) The fundamental theory of flame suppression by halons is still very unsettled despite the use of halogen based extinguishers since 1907. 2) Thus far all gaseous substitutes are less effective than halon 1301. 3) Some progress has been made in gathering reaction rate data that might eventually help provide the basis for a kinetic theory of fire suppression when halogens are the active agent. 4) Lack of success with gaseous agents enhances the incentives to drive home an aerosol suppressant approach. 5) Particulates in the form of finely ground powders of selected chemicals have been used for fire suppression for over four decades. The most accepted theories as to their action invoke thermal mechanism. 6) In view of the large thermal heat release in proposed PGS devices cooling the pyrotechnically generated particulates or gases should be critical to their successful use as fire suppressants. 7) If free radical scavenging can play a major role the cooling, weight and size requirements should be more modest. 8) Clearly we would make more rapid progress in developing halon alternatives, particularly PGS systems, if the basic physical and chemical mechanisms involved in fire and fire suppression were better understood.

Among existing attempts to explain fire suppression the Thermal (TH) approach of Ewing et al.[2] correlates flame extinction by halons and particles with heat capacity and endothermic reaction sinks. On the other hand the Free Radical (FR) approach of Westbrook [3] invokes scavenging of OH, O, H and other free radicals to interrupt the important fire sustaining chain reactions. The fact that these contrasting approaches have still not been reconciled [1] is a sad commentary on fire suppression research over the decades.

In our experimental attempts to resolve the serious difference between the TH and FR approaches we have used total radiation measurements, visible spectroscopy and particularly Middle Ultraviolet Spectroscopy (MUV). MUV spectroscopy appears to be a particularly valuable tool because of its sensitive capability of displaying OH emissions [4-8]. We have attempted to identify mechanisms of flame suppression of gas burner flames and liquid hydrocarbon pool fires by halons and PGAs using MUV spectroscopy [9-12]. To use MUV spectroscopy in flame suppression studies one must pay careful attention to the large Visible (V) and near Infra Red (IR) emissions of smoky fires. When stray VIR light is reduced one can obtain significant information about free radical processes that should be helpful in assembling a complete theory of hydrocarbon flame suppression. Figure 1 shows an early CCTL experimental arrangement designed to deliver a known volume rate of aerosols to a fuel zone. Figure 2 shows the MUV spectra of a heptane flame using our computer-spectrometer and a standard visible blocking filter with and without aerosol suppressant [9]. The large sharp features in 2a around 308 nm are OH emissions that are greatly reduced in 2b when SFE aerosols are added. These observations reinforced our focus on OH scavenging mechanisms.

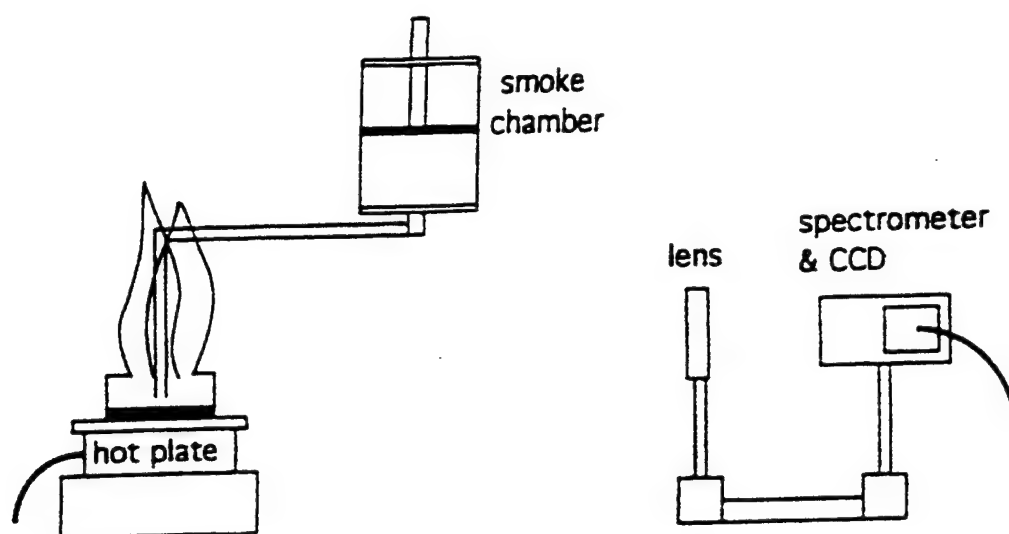


Figure 1. Experimental Arrangement for Spectroscopic Analysis of Pool Flame with Aerosol Suppressant

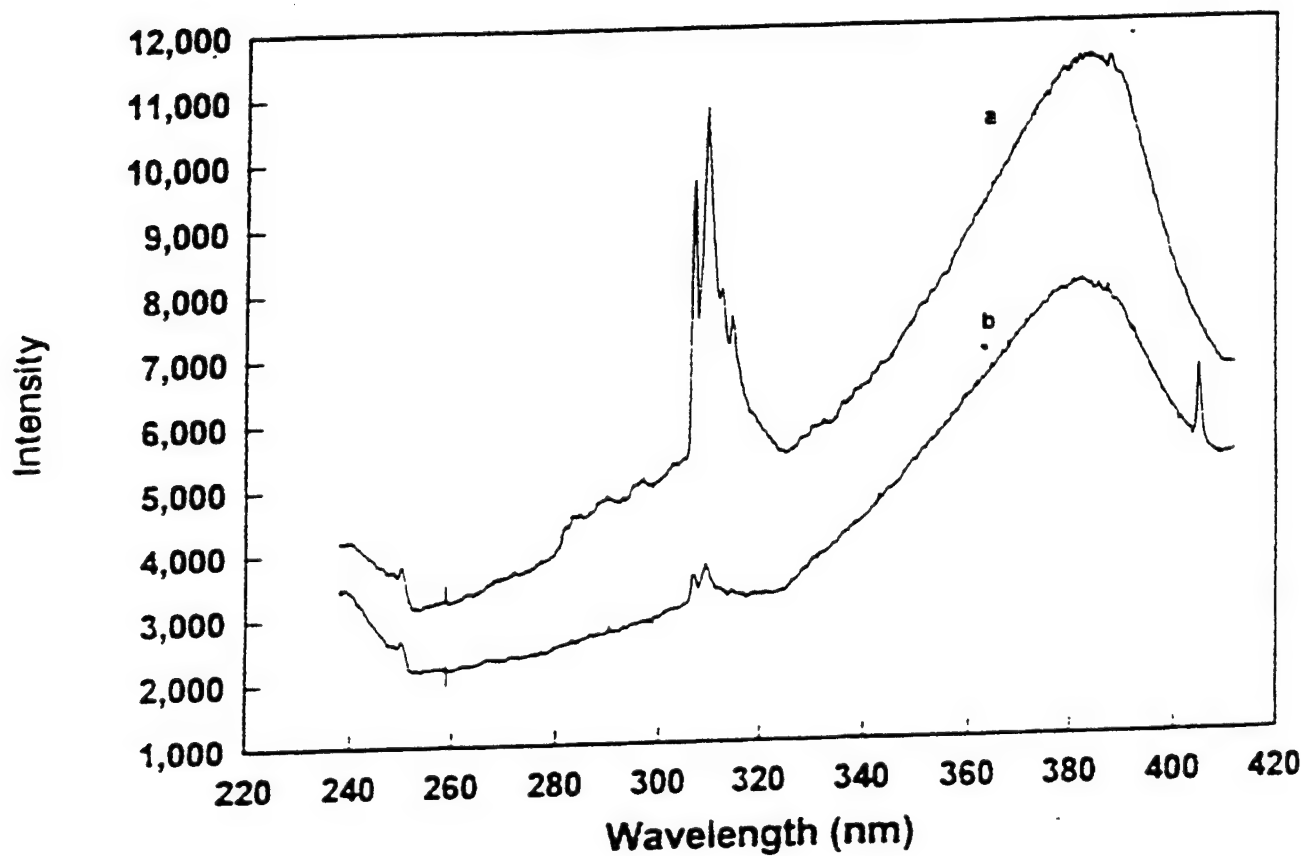


Figure 2. Heptane and Aerosol Suppressant. (a) No suppressant , (b) Aerosol added.

## SECTION II

### FLAME SUPPRESSION AND HEAT ABSORPTION STUDIES

#### A. PRIOR PYROTECHNICALLY GENERATED SUPPRESSANT (PGS) WORK

There is a considerable background in pyrotechnically generated aerosols (PGA) [13]. Our focus is on PGAs being developed by Spectronix Ltd. whose characteristics have been described in a number of recent reports [14-17]. Methods of cooling these aerosols in stationary generators have also been reported [18]. The cooling and flame baffling requirements for throwable PGA devices are much more difficult than those for stationary systems. Pyrotechnic charges developed by the Spectrex Corporation will be referred to as Spectrex Fire Extinguishant (SFE) and three solid formulations have been available to us (A, B, and C) and two powdered formulations (A and B). The heating values as measured with our Parr calorimeter are listed in Table 1.

During our tests to date we have ignited some 250 SFE charges in masses ranging from the one gram level to the 500 gram level in various arrangements and devices. We have mainly used an ignition system consisting of a fine tungsten wire and a battery or DC power supply of six to twelve volts. Many of the smaller tests were made in connection with flame suppression studies on laboratory scaled fires. The larger firings have mostly been in connection with testing of cooling mechanisms intended to be helpful to the design of hand thrown PGA devices.

The practical utility of a PGA device is largely dependent on the effectiveness of the systems utilized for cooling the aerosols and for baffling the exhaust so that no flame escapes. The flame from the SFE which burns at temperatures greater than 2500 K, could cause secondary fires if it escapes the device. A low smoke temperature is desired to keep the overall compartment temperature from rising to unacceptable levels and so that the smoke will stay closer to the floor instead of rising to the ceiling, away from the combustion zone. On the other hand, cooling the burning PGA material and aerosols must not interfere with the aerosols fire extinguishing characteristics. Particle deposition and dilution of the smoke must be minimized and the composition of the smoke should not be altered so as to reduce its effectiveness.

The heat released in the combustion zone of burning PGA material is dissipated in radiation, convection and conduction between the products and the chamber walls and in the thermal capacity of the products. Experiments with Spectrex Fire Extinguishant (SFE) have shown that excess cooling of the combustion zone itself can significantly increase the burn time and possibly lead to quenching or incomplete combustion-both of which are undesirable. Thus we have mostly burned the SFE in an insulated combustion chamber so that it would approach adiabatic conditions.

Post combustion chamber cooling can be achieved by the transfer of heat between the products and the passageways external to the combustion zone but internal to the device. This can lead to storage in the device through the thermal capacity of materials or through a phase change of heat absorbing materials. Table 2 shows the thermal properties of some common liquids and metals that might be used to absorb heat in possible SFE based devices. Table 3 gives the dissociation temperatures of some ceramic materials that could be used in high temperature energy absorption.



Table 1. Heating Values of SFE as Measured with a Parr Calorimeter (in BTU/lb)

SFE Type	Pellets	Powders
A	2223	2028
B	2202	2157
C	2917	N/A

Table 2. Thermal Properties of Common Materials

Material	Specific Heat (kJ/kg.°C)	Density (kg/m <sup>3</sup> )	Thermal Diffusivity (m <sup>2</sup> /s) x 10 <sup>6</sup>	Thermal Conductivity (W/m.K)
water (liquid)	4.2	1000	0.14	0.613
steel	0.43	7800	17.7	60.5
aluminum	0.90	2700	97.1	237
copper	0.39	8900	117	400
brass (70/30)	0.39	8500	33.9	110
ethylene glycol	2.4	1100	0.09	0.252

Table 3. Dissociation Temperatures of Ceramic Materials

Adapted from Ceramic Glazes by C. W. Parmelee, Industrial Publications, Inc. Chicago 3, Ill. 1951

Compound	Temperature	Remarks
Clay.....	405°-850°C.	Chiefly at ca. 450°C.
Calcium carbonate*.....	886°-915°C.	Depending on the grain size can be as low as 610°C.—Turner.
Sodium nitrate.....	Decomposes slowly below 540°C.	Depends on rate of heating. The m.p. is 308°C. $2\text{NaNO}_3 \rightarrow 2\text{NaNO}_2 + \text{O}_2$
Magnesium carbonate.....	Between 800°-900°C.	
Dolomite.....	-----	Two stages: magnesium carbonate decomposes first, later the calcium carbonate.
Potassium carbonate.....	Above 1100°C.	M.p. is 894°C.
Potassium nitrate.....	-----	M.p. is 333°C.
Sodium carbonate*.....	Above 1750°C.	M.p. is 851°C.
Sodium nitrate.....	-----	$2\text{NaNO}_3 \rightarrow \text{N}_2 + \text{O}_2 + \text{Na}_2\text{O}$
Boric acid.....	-----	Decomposes in 2 stages: boric acid dissociates, dehydrates before 200°C.; all water is out at 900°C., decomposes at 1400°C.

\* Sodium carbonate and calcium carbonate react to form  $\text{Na}_2\text{Ca}(\text{CO}_3)_2$  at about 800°C. and this melts at 813°C.

Given that the aerosol generation occurs rapidly the conductive properties of the metals, particularly copper and aluminum, look most attractive. However, the specific heats of these metals are not as high as that of water. In addition, water has a very high heat of vaporization (2257 kJ/kg or about 970 BTU/lb). These properties make water a far more efficient heat absorber from a mass standpoint than the metals. A drawback of water is that its thermal conductivity is low and hence it might be difficult to utilize its high latent heat during the SFE burning time constraint.

Recognizing the complexity of the heat transfer processes that might be used for post combustion zone cooling we have adopted the philosophy of building or adapting simple prototype devices in a search for promising general arrangements for cooling SFE generated aerosols and baffling the flames. The intent was to find an approximate solution experimentally and then to optimize this solution by mathematical modelling.

## B. CHARACTERISTICS OF SFEs

To design a hand-thrown EMAA (SFE) device that would inhibit the amount of "flame" leaving the canister, one must determine the normal temperature, burning velocity, and other thermal characteristics of SFE combustion. This information will aid in predicting the characteristics of practical devices. In our Task 3.06 studies we have established procedures for burning 1-5 gram quantities in our available laboratory hoods in our Space Sciences Building laboratories. We also have shown that pan fires that can be accommodated by our 3rd floor SSRB laboratory hoods can be extinguished by the particles from 1-5 gram SFE pellets. Subsequently we fired 20 gram SFE pellets in our 3rd floor hoods and established that such firing can be carried out safely. Working from the Penthouse on the Space Sciences Research Building we developed safe procedures to investigate the flame characteristics of 100 and even 200 gram pellets. Accordingly flame propagation of the SFE material were studied in the laboratory to obtain a better understanding of flame temperature, normal burning velocity of the powder or pellet, burning velocity as a function of pressure, ignition temperature, heat of combustion, etc. These studies were intended to give us practical design information for the development of cooling and flame retention methods.

Among the provocative concepts that came out of our exploratory studies under Task 3.08 was the possibility that radiative cooling might be useful in getting rid of the energy of our pyrotechnic generator of fine particles. In our exploratory pan fires we rarely reached temperatures in excess of 1600°F (1144 K). In these cases we estimate that the radiation power losses/combustion power can be of the order of 0.25 or 25%. This figure is compatible with 25-40% range for pool fires given in the literature. In estimating the temperature of 20 gram SFE-A pellets we concluded we had reached temperatures from 2500° - 3000°K. This estimate was based upon our comparison of the normalized Planck spectrum obtained by examining a 1000 watt tungsten halogen lamp filament at full power with the observed filament spectrum at reduced power levels. Figure 3 gives spectra from an SFE burn and the filament spectra at currents of 8.5, 7.5 and 6.5 amps all normalize to the same peak count rate and observe through our Schott filter. The fact that the SFEs peaks at shorter wavelengths suggests that its burning temperature is of the order of or exceeds 3000°K.



There are a number of possible sources of error in this novel temperature measurement scheme, including the light leaks in our Schott filter in the red and infrared. However even granting an SFE-A burn temperature of only 2500 K, that is quoted in the literature we would expect from the Stefan Boltzmann Law ( $R = \sigma T^4$ ) that the radiative power loss/combustion power is far greater than that of pan fires and that it probably exceeds 50%. These observations suggested that we should investigate practical cooling arrangements that permits the direct escape of the SFE-A radiation during the smoke generating process but restrict the paths of the flame and combustion gases for further cooling by other mechanisms.

### C. SINGLE CHANNEL STUDIES

Solid particulate aerosol fire suppressants undergo pyrotechnic combustion and flames are generated as a direct result of the combustion process. In connection with our studies on Task 3.06 "Thermal Performance of Solid Particulate Aerosols" and sub-task 2 of Task 3.08 we initiated a number of efforts to quantify the delivery of SFE aerosols to various well defined pool fires. The idea was to make smoke from SFE, cool it, establish the density of the smoke, and to deliver the smoke at known densities and volume rates to well defined pool or burner fires.

To study extinguishment characteristics of SFEs on a laboratory scale we have conducted many tests with simple arrangements intended to generate the aerosols and attendant gases, cool them and deliver a known amount to a burner flame or pool flame. In some of these efforts we used pool fires with diameters 2 inches, 4 inches, and 6 inches and sought features of effective pool fire extinguishment techniques. The devices used to generate the aerosols will be referred to as single channel devices. These single channel studies also provided reproducible cases to examine the radiation and spectra of SFE aerosol interactions with burner and pool fires [9]. Towards these ends we examined the three aerosol generator delivery systems described below.

#### 1. Cylinder and Piston

The concept of the SFE delivery arrangement schematically illustrated in Figure 1 was to fire the SFE and have the products of combustion (smoke) fill a prescribed volume, in this case a cylinder about 6" in diameter and 12" tall. We then ejected the smoke at a desired volume rate with a weighted piston. Glass and plastic cylinders from discarded anesthesiology machines were used. The piston was weighted but restrained to fall at a prescribed rate using a pulley arrangement coupled to a precision linear driving device. Figure 4 illustrates the final piston-cylinder device. Some problems were encountered with sticky piston rings but these could be dealt with by periodic cleaning and light lubrication.

To deliver the smoke output to pool fires in the chemical hood we used a metal pipe with a fan shaped opening directed so the aerosols covered the fire. We developed simple firing chambers and ignition systems and valve arrangements to first load the cylindrical chamber with aerosols. Then with the piston lowering we would direct the output to the pipe reaching the pool fire in the hood. We had some difficulty with this arrangement in delivering enough aerosols to quench all but the smallest pan fires. During this experimentation we found that when we valved the system so the smoke went directly from the firing chamber to the delivery pipe (rather than to the cylinder) we could quench pool fires with very small charges.

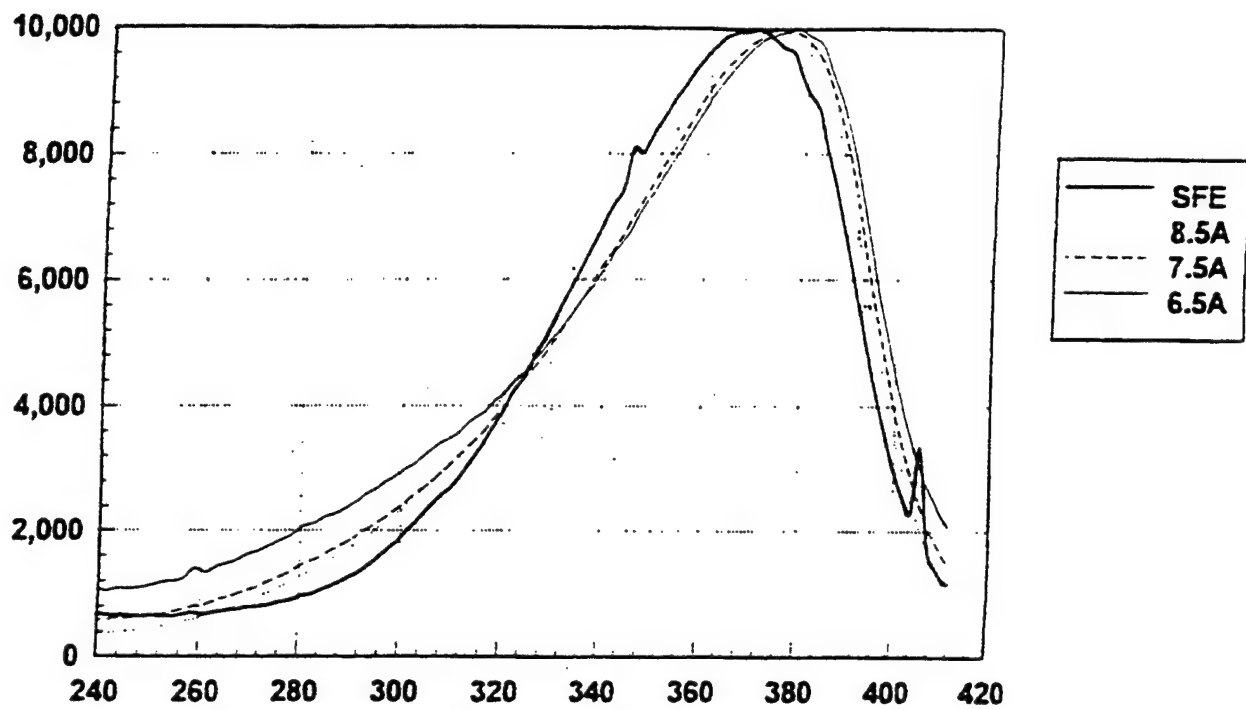


Figure 3. Modified Wien's displacement law estimate of SFE combustion temperature.

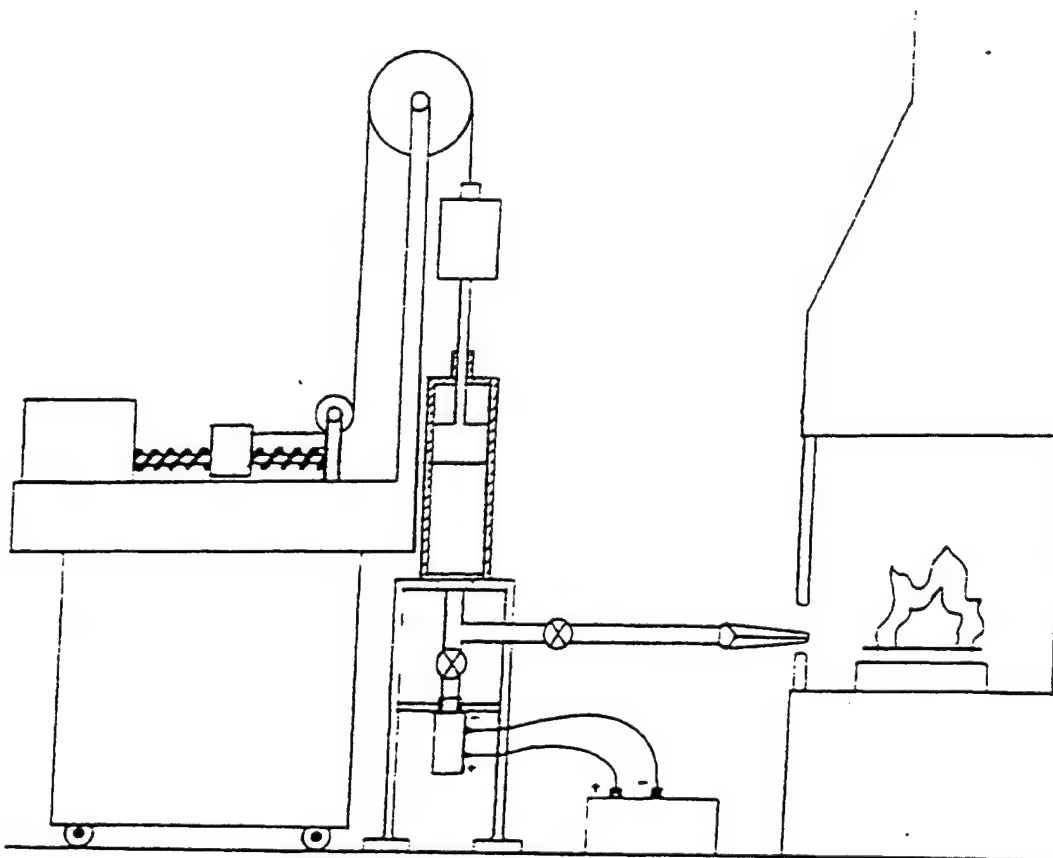


Figure 4. Final piston - cylinder device.

Furthermore it was simple to cool the aerosols exiting our pipe. This experience was helpful in the evolution of our firing mechanisms, our single channel studies and in learning how to deal with increasingly larger SFE charges.

## 2. Bell Jar

Before developing the cylinder-piston arrangement. We made use of an available bell jar having volume of about 3 cu.ft. We burned a known weight of SFE inside the jar allowing the products of combustion to displace most or all of the air and to cool. We provided means of circulating the aerosol products of combustion. To force the aerosols out of the jar through a 1/2" diameter hose. We added water at a known rate to a container inside the bell jar, knowing the pressure inside the jar. A variation of this equipment considered was to build up the pressure inside the jar and release the aerosols to the "fire" at higher velocity while recording the pressure change with time.

This approach was abandoned due to several problems with sealing the jar and replacing and firing the SFE charge, the weak displacement of particles by the water system and concern that the aerosols would stick to the tubing connecting the jar to the area of the fire.

## 3. Syringe Apparatus

The precision linear translation device used above was built for injecting liquids with 50 cc syringes at various prescribed rates. We also tried using the syringe device directly to deliver aerosols at various known rates between about one and 3.8 cc/minutes. This approach was dropped due to small total volume of the cylinders and the low velocity feed rate of the smoke.

In addition to the extinguishment characteristics of interest we used these studies to examine mechanisms for cooling the SFE aerosols. Our findings indicated that metallic pipe 2 or so feet long could cool the aerosols from 20 gram SFE charges by heat conduction, low temperature radiation and convection. Covering the outside of the pipe with wet cloth was an effective way of enhancing the cooling. In the course of pursuing this line of investigation the possibility of using a single channel or a double channel device directly as a fire extinguisher suggested itself. This will be discussed in the section on potential off-shoots of this effort.

In our small scale tests with single channel devices we investigated a variety of cooling systems that were later applied in multichannel form in our efforts to develop a 500 gram SFE throwable device. Various water saturated ceramic lined passageways and metal tube heat exchangers were utilized. In tests conducted in the laboratory hood, a device constructed with a cooling passage made of coiled copper tubing was successful in extinguishing a 6" diameter heptane fire using as little as 10 grams of SFE.

Several of the single channel devices we tested incorporated both metals and water to absorb energy. By using a multichannel heat exchanger in which the passages have a high surface area to cross-sectional flow area ratio, the response of the water can be speeded up considerably. When using water in passages it must be vented to release the steam or to generate a fine mist. When water is used for cooling, water absorbing and retention materials are, of course, needed.

In tests with full scale or half scale devices we found thus far that water was the most promising heat sink in terms of rapid and large absorption of the heat of SFE combustion. Whether the water vapor that could accompany the aerosol in some arrangements assists or detracts from the fire extinguishment properties became a question. Using a single channel device against laboratory scale pool fires provides the simplest way of testing the influence of the added water vapor. Should the influence be substantially negative it would be important for the national pyrotechnically generated suppressant project to seek other sources of aerosols with substantially reduced heat generation. Alternatively it would strongly influence the type of heat absorber we focus on in our design of a practical full scale device. If water vapor improves the fire extinguishment properties we could foster its generation in final designs. Thus far we have not observed an adverse effect of water vapor upon the small pool fire suppressing ability of SFE generated aerosols.

It is our understanding that water vapor was used in conjunction with the exhaust of a jet engine to extinguish oil fires (well head) in Kuwait after Desert Storm. Steam is also used for cooling the latest high temperature gas turbines in the drive to break the 60% barrier in combined cycle electrical generation systems. Steam is also used in recent high efficiency drying systems. Accordingly we have given serious attention to water based cooling of SFE aerosol generating devices.

#### D. OVERVIEW OF MULTICHANNEL DEVICES

Among our 250 plus PGA tests we have recorded over 90 experimental device firings on videotape. Appendix A gives a listing and brief description of the devices tested that are recorded on videotape. Acronyms for approaches for cooling and flame retention of a 500 gram SFE charge that appeared potentially viable are:

1. (MWCD) SFE

(MWCD) SFE aerosol cooling through multichannel water embedded and sealed ceramic passageways leading to a cooled wet aerosol (designated Multichannel Wet Ceramic Device).

2. (MFTB) SFE

(MFTB) SFE aerosol cooling via a multichannel fire-tube boiler system leading to a cooled dry aerosol and a separate steam exhaust (designated Multichannel Fire Tube Boiler).

3. (CHRD) SFE

(CHRD) SFE charge with dolomite or other low dissociation temperature carbonates added to absorb and retain heat while generating CO<sub>2</sub> with the aerosols (designated Carbonate Heat Retention Devices).

4. (RCBD) SFE

(RCBD) SFE flame radiation cooling through mica like windows with baffling for the flame and multiple passageway cooling for the aerosols (designated Radiative Cooled and Ruffled Device).

### SECTION III

#### WET CERAMIC DEVICES

##### A. THE JANUARY 12, 1995 DEVICE

On Thursday, January 12, 1995 we succeeded, essentially by a multichannel approach, in dissipating practically all the heat from a 500 gram SFE charge within a one gallon container heat sink-SFE source. The smoke was cooled below the ignition temperatures of all common materials and no fire escaped the container. The January 12 device used light weight ceramic materials provided by Bruce Green, a local commercial potter. Figures 5 illustrates this device.

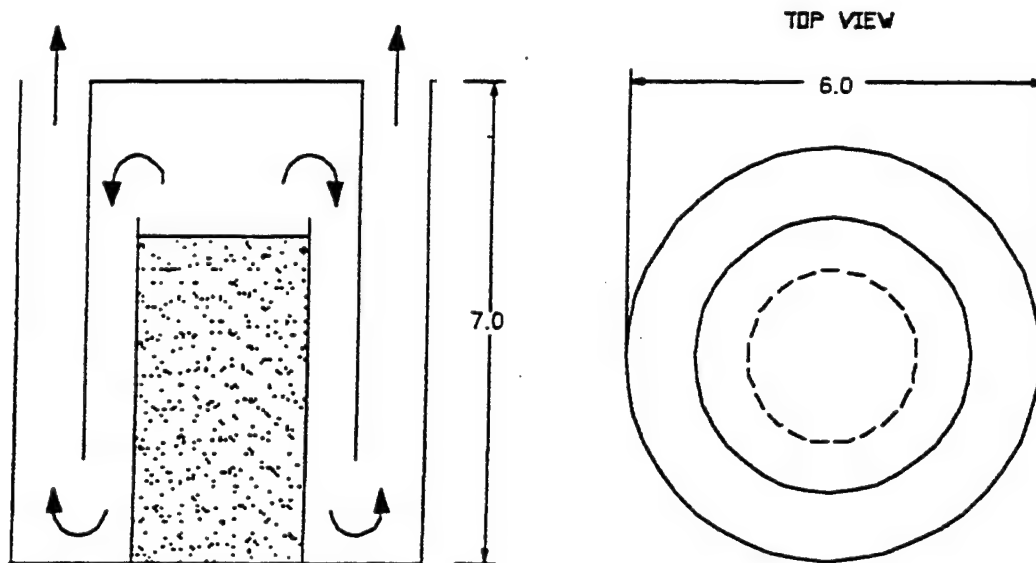
The canister had sufficient heat absorbing material such that the exhaust gases were below 200° C or 390° F and the total weight of the canister was about six pounds. The 500 grams of SFE material burned uniformly for approximately 1.75 minutes emitting a dense 6 inch diameter column of low velocity aerosols. The possibility of exiting finally through a metallic radiator heat exchanger was also considered but was not used. Such a final passageway might also be pursued if further cooling is needed. One can anticipate that the inclusion of a light weight radiator heat exchanger will further lower the exhaust temperature to 100° C or below.

Several other modifications can be made to improve upon this prototype that demonstrated a multichannel approach of burning 500 gms of SFE and absorbing sufficient energy that the exhaust aerosols and the container would not re-ignite "class A materials." We appeared to be converging to a potentially useful realizations of heat transfer - heat absorption combinations that would point the way to small practical systems. At that point we could fabricate a potentially throwable 500 gram SFE device, of 6-8 pounds and a gallon sized container.

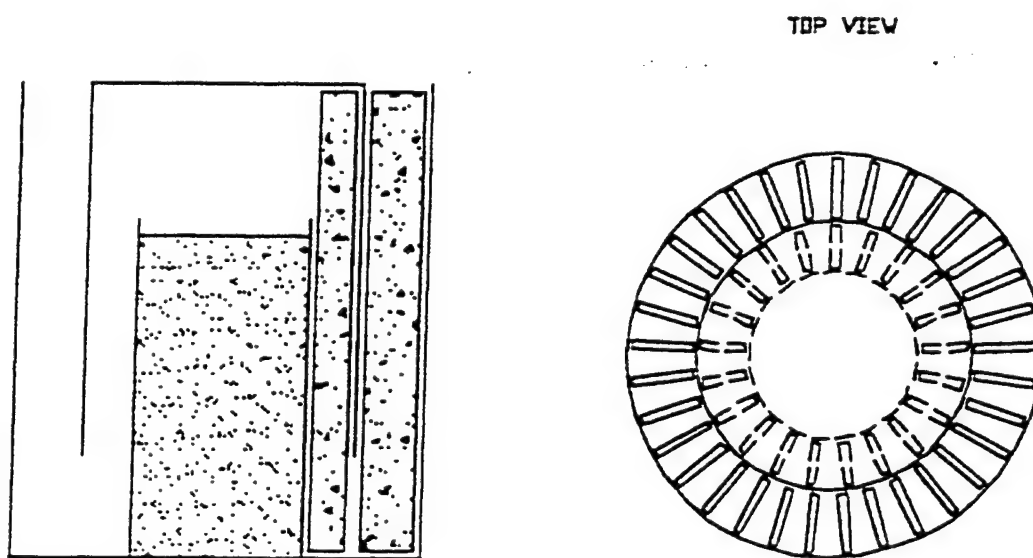
The MWCD is essentially built around the concept of utilizing water as a primary cooling agent. Because of its low thermal conductivity, the water used for this application must have a relatively large surface area to be effective. To increase the available surface area this device convolutes the exhaust path and subdivides it into many channels by using partitions that are capable of holding water.

To implement the concept, a series of three descending-size metal containers are stacked inside each other to extend the path through which the aerosol must travel. The innermost container holds the SFE charge, and the exhaust is directed outward against a layer of high-temperature insulation "wool" lining the top of the middle canister. Additional lined surfaces are used on the outer circumference of both the inner can and the middle can. These surfaces were covered with a woven version of the high-temperature insulation which is also capable of holding water, although not a large percentage. The cooling of the aerosol is primarily achieved by the addition of a porous refractory (to greatly increase the surface area of the exposed water) material shaped into thin rectangular partitions which are arrayed around the circumferences of the inner and middle canisters.

There were 54 fin sections total, 21 along the inner ring and 33 along the outer ring in the January 12th device. As the aerosol stream moves past the fins, the water absorbs heat and changes phase into steam; the steam mixes with the aerosol and



Multichannel Device (MWCD). Aerosol Path Detail.



Multichannel Device (MWCD). Fin Placement Detail

Figure 5: Schematic Diagram of the Multichannel Wet Ceramic Device (MWCD)

passes out of the device. Together, the fins were capable of holding approximately 500 grams of water, which if converted completely to the gas state would absorb over 1000 Btu. Total weight of the prototype was around 3 kg (6.5 lb). Since the refractory material used to create the fin sections is inherently fragile, alternative materials have been obtained that might serve the same purpose and also be able to withstand shock.

The results from a test firing of a 500 gram SFE charge showed a maximum exit aerosol temperature in the range of 200 °C, along with an elapsed burning time of 1.75 minutes. The ceramic multichannel device was essentially built around the concept of increasing the effectiveness of water as a cooling agent. We had not yet had the opportunity to develop a complete mathematical model for the multichannel form of heat absorption device. It is clear, however, that the material used to retain water is important to the success of this approach.

## B. MATERIALS FOR MULTICHANNEL DEVICES (MMCD)

Various materials and fabrication techniques have been considered for water retention and delivery in MWCDs from the standpoint of their specific heat, heat of vaporization if applicable, heat of dissociation, heat of dehydration, shock tolerance, etc. Small scale trials have been conducted using limestone, dolomite, boric acid, borax and clay near the burning zone based on their very high absorption of energy at high temperatures. At this time water appears to be the most practical heat absorber for the majority of the energy released by the SFE because its low boiling point and high heat of vaporization permits rapid heat absorption. The following are the materials that we examined to utilize these properties of water:

### 1. Clay Extrusions

Bruce Green has provided equipment to extrude refractory tubes of various shapes that can be used to make multiple passages for the SFE smoke. The tubes can be of various clay compositions and fired so as to have high degrees of porosity. These porous portions will contain water if water is the best heat absorbing material and does not adversely impact the fire extinguishment qualities of the SFE aerosols. The degree of porosity will be governed by the clay mixture with material that will "burn out" when fired and the firing temperature. The size, number of channels and surface configuration will determine the pressure drop, surface area, and the rate of heat transfer to the absorbing media.

### 2. Fiberfrax

Experiments using bulk fiberfrax might also be conducted where the fiberfrax would be molded in various configurations to give the required surface area to the SFE exhaust and in addition hold sufficient water as the heat absorber. The fiberfrax can be stiffened as needed with various materials such as colloidal silica, clay, etc.

### 3. Woven Fiberfrax

Woven fiberfrax cloth might also be tried alone or in combination with any of the other techniques. Inconel wire enmeshed cloth might be examined also to improve strength and heat conductivity.



#### 4. Fiberfrax Paper

For some disposable applications fiberfrax paper may be adequate for water retention, fire resistance and good conduction.

#### 5. Coated Wire Screen

Wire screen, (Aluminum, Copper and Steel) were tried in various configurations to control the exhaust gas path as well as provide large surface areas and high thermal conductivity to the water or other material for heat absorption. The wire mesh or screen was coated with materials such as clay, borax and limestone, all three having high energies of dissociation and/or high water of hydration. The results did show promise when using 20 grams of SFE.

#### 6. Clay Plug

This approach would be to drill and shape a clay form to give a large surface area for the gases to scrub as they exit and in this way transfer energy and heat to the clay that has water entrapped. If the clay ( $\text{Al}_2\text{O}_3 \cdot 2.25\text{iO}_2 \cdot 2\text{H}_2\text{O}$ ) is dried at low temperatures it will still have heat absorbing qualities via its water of hydration.

#### 7. Porous Metallic Fins

Metal shavings formed into fins might be tried with water filling the voids. The rationale is that with the fins one can create a large surface area exposed to the hot gases from the SFE. The fins being metal (preferably Al or Cu but steel might do) will transfer the heat into the center of the fin and thereby transfer the energy to the water trapped in the fin. This will transfer the energy hundreds of times faster than the heat transfer using water alone or water held by a refractory.

#### 8. Stabilized Water

Water draining to the bottom of the container with time is a potential problem with water based heat absorber systems. To reduce this effect the water needs to be held in place possibly by an additive that would "thicken" it or gel it. Various thickeners might be tried and evaluated in conjunction with items 5, 6 and 7 above.

#### 9. Water Sealants

Sealants that are quickly vaporized at high temperatures permitting vaporization of entrapped water in one of the refractory matrices described above might be tried. The WET-PAK refractories provided by Carborundum Corp. or other ceramic companies that only harden after a high temperature firing might be suitable.

#### 10. Metal - Ceramic Composites

A new class of materials that combines the high temperature capabilities of ceramics and the high conductive properties of metals might be tried. By using composites with some of the water absorbing and sealing characteristics mentioned above sufficiently rapid passageway cooling might be achieved.



## C. CERAMIC CHANNEL STUDY - HEAT TRANSFER ANALYSIS

### 1. Introduction

In our previous SFE firings with various cooling devices and cooling mechanisms, the most promising results were achieved with a multichannel wet ceramic device. This device was composed of three concentric cans, with the center can containing the fuel and the flow areas being annular regions between the cans. The annular regions were divided into channels by ceramic fins. The device had two stages, the second stage was a concentric annular area around the first (See illustration in Fig. 45). This device, the size of a one-gallon can and about six pounds in weight, was able to contain the flames and cool the exhaust of 500g (1.1 lb) of the SFE material (which released about 2.9 MJ in the 1 minute 40 second burn time) down to about 70 °C one foot away from the exit of the device. The following is an investigation in which a model of the flow of the SFE exhaust through a ceramic channel is developed so that an analysis may be performed as to whether these results can be achieved in a smaller, lighter device. This model considers channel size, shape, and the number of channels necessary to achieve optimum performance, as well as the issue of the ceramic drying out before the burn is complete.

### 2. Symbols

$A_c$  = Cross Sectional Channel Area  
 $A_p$  = Single Slice "Wetted" Channel Perimeter Area  
 $C_p$  = Specific Heat of Exhaust at Constant Pressure  
 $D_h$  = Hydraulic Diameter =  $4A_c/P$   
 $h$  = Average Convection Heat Transfer Coefficient of Exhaust  
 $k$  = Average Thermal Conductivity of Exhaust  
 $m$  = Average Mass Flow Rate of Exhaust  
 $\mu$  = Fluid Viscosity  
 $Nu$  = Nusselt Number =  $hD_h/k$   
 $P$  = Channel Perimeter  
 $Pr$  = Prandtl Number =  $C_p\mu/k$   
 $Re$  = Reynolds Number =  $\rho V D_h/\mu = 4m/\pi D_h\mu$   
 $\rho$  = Fluid Density  
 $T_n$  = Exhaust Temperature (at nth location)  
 $V$  = Average Velocity of Exhaust

### 3. Modeling the Ceramic Channel

The model of the heat transfer through the ceramic channel was based on the transfer of the thermal energy of the hot aerosol exhaust to the water in the ceramic walls of the channel. This heat exchange is described by an energy balance that equates the heat which is lost from the hot exhaust (via convective heat transfer to the ceramic walls) to the reduction in internal energy of the hot exhaust. This equation was used in conjunction with a ceramic tube which was discretized into thin slices. It was assumed for this model that the ceramic would stay moist for the duration of the burn so that the temperature of the ceramic tube would reach but not exceed 375K. The model assumed a steady state condition where each slice was isothermal (i.e. the gas at each slice is at a uniform, constant temperature); thus, the heat lost through convection in one slice predicts the temperature of the gases in the next slice. Shown below is the energy balance which corresponds to the discretized tube.

$$hA_p(T_n - 375) = mC_p(T_n - T_{n+1}) \quad (1)$$

The left-hand side of the equation is the heat lost from the exhaust due to convective heat transfer with a slice of the wet ceramic walls, and the right hand side of the equation represents the decrease in internal energy of the exhaust from one slice to the next. The parameters which need to be determined are the average overall convection coefficient ( $h$ ) through the channel, the exposed wetted perimeter area of each slice ( $A_p$ ), the mass flow rate per channel ( $m$ ), and the average specific heat ( $C_p$ ) of the exhaust. The convection coefficient is obtained from the definition of the Nusselt number ( $Nu = hD_h/k$ ). The Nusselt number is a function of the Reynolds number ( $Re$ ), where for laminar flows  $Nu = 3.66$ , and for turbulent flows the correlation  $Nu = 0.023Re^{4/5}Pr^{0.3}$  is used [19]. Thus, for turbulent flows, the Prandtl number ( $Pr$ ), must also be determined. The Reynolds number is a function of the mass flow rate ( $m$ ), the average viscosity ( $\mu$ ) of the exhaust, and the hydraulic diameter ( $D_h$ ) of the flow channel. If these parameters are known, and if the temperature at the inlet ( $n=0$ ) is known, then the temperature of the exhaust at all other slices may be determined. Rearranging Equation 1, we obtain:

$$T_{n+1} = T_n - (hA_p(T_n - 375))/mC_p \quad (2)$$

In this way, the model can be used to predict the exit temperature of an exhaust stream for a variety of different flow configurations. As shown in the above equation, the cooling can be greater for larger values of the quantity  $hA_p/mC_p$ . The value  $h$  is much greater for turbulent flows than for laminar flows, and increases as the turbulence increases. As the mass flow rate increases through a channel, the flow will transition to turbulence and become increasingly turbulent. Thus, the value of  $h/m$  will be maximized near the onset of turbulence where the mass flow rate will be low but the convection coefficient will be high. The value  $A_p$  represents the wetted surface area in contact with the exhaust, which depends on the selected geometry of the channel.

#### 4. Testing the Model

##### a) Multichannel Device

The first test of the model was performed for the multichannel ceramic device which utilized ceramic fins to divide the flow into separate channels with the intent of exposing the exhaust to a greater wetted surface area. The multichannel device was contained in a one gallon can, and was separated into two stages as shown in Figure 5. Each stage was an annular region between concentric cans. The first stage was the region between the fuel can (approx. 2.63 inch diam.) and an intermediate can (approx. 4.25 inch diam.), and the second stage was the region between the intermediate can and the outer can (approx. 6 inch diam.). From the fuel can the exhaust must undergo an 180-degree turnaround to flow through the first stage, and then another 180-degree turn around to flow through the second stage. The annular regions were divided into channels with the rectangular ceramic fins. The first stage fins were about 1.5 cm wide by 0.4cm thick and 17cm long. The second stage fins were about 2cm wide by 0.4cm thick and 17cm long. The first stage was divided into 21 channels, and the second stage 33 channels. This device used 500g of the SFE powder, which burned in about 100 seconds and yielded a peak outlet temperature of about 180C. The average flow rate then is about 5g per second which

is divided into 21 first stage channels and 33 second stage channels. It was assumed that the flow was distributed equally through all of the channels in each stage. The first stage channels had a cross-sectional area of about  $1.94 \text{ cm}^2$  ( $D_h = 1.4 \text{ cm}$ ) and the second stage channels had a cross-sectional area of about  $1.77 \text{ cm}^2$  ( $D_h = 1.2 \text{ cm}$ ).

In order to model the device it was necessary to determine values for the unknown SFE exhaust parameters of thermal conductivity, specific heat, and viscosity. The composition of the exhaust products were known to be approximately 60% gaseous ( $\text{O}_2$ ,  $\text{N}_2$ ,  $\text{CO}_2$ , and  $\text{H}_2\text{O}$ ) and 40% solid particles ( $\text{KCl}$ ,  $\text{K}_2\text{CO}_3$ ). Since all three of these parameters vary with temperature and the analysis is to be performed over a wide temperature range all of the parameters were estimated from an approximate average exhaust temperature of 1700K. The gaseous constituents have a thermal conductivity of about  $0.1 \text{ W/mK}$  at 1700K. The solid particles were assumed to have a thermal conductivity of about  $0.15 \text{ W/mK}$ . Therefore, based on the 60/40 gas to solid ratio, the conductivity of the aerosol exhaust was approximated as  $0.12 \text{ W/mK}$ . The specific heats of  $\text{O}_2$ ,  $\text{N}_2$ , and  $\text{CO}_2$  are about  $1270 \text{ J/kgK}$  (approximated as air at 1700K), and the specific heat of water vapor is about  $2000 \text{ J/kgK}$  at 1700K. The specific heats of  $\text{KCl}$  and  $\text{K}_2\text{CO}_3$  at 1700K are about  $730 \text{ J/kgK}$  and  $1000 \text{ J/kgK}$ , respectively. It was assumed that the gaseous products were in equal amounts and the solid products were in equal amounts to yield an average gaseous specific heat of  $1333 \text{ J/kgK}$  and an average solid specific heat of  $865 \text{ J/kgK}$ . Thus, based on the 60/40 split, the overall specific heat of the exhaust was approximated as  $1150 \text{ J/kgK}$ . The viscosity of the exhaust was approximated as that of air at the average temperature of 1700K, being about  $370 \times 10^{-7} \text{ Ns/m}^2$ . It should be noted that this value may be low due to the 40% solid particle composition. The flow rates yield Reynolds numbers of about 620 for the first stage, and about 540 for the second stage. Thus, laminar flow was assumed for the model, and a Nusselt number of 3.66 was used in determining the convection coefficient. For the SFE firings, it is assumed that the burn temperature is on the order of 3000K, and this value was used as the inlet temperature.

Figure 6 is a plot of the predicted temperature vs. distance profile along the length of the flow path. The middle plot shows the model's results for a hypothetical continuously wet device, the top plot accounts for dry-out of the first five centimeters of the ceramic (we observed dry-out of approx. the first 5cm of the channels), and the bottom plot assumes a 1000K inlet temperature for comparative purposes. As shown in the graph, the model which accounts for the dry-out predicts an outlet temperature of about 550K, or about 280C, whereas the actual maximum outlet temperature was about 180C. Thus, the actual device performed better than what the model predicted since the actual device cooled the exhaust an additional 100C. The plot in Figure 6 shows that the heat flux is greater (steeper slope) for higher exhaust temperatures. The curve which was plotted for a 1000K inlet temperature, although 2000K cooler, has comparable exit temperatures with the 3000K inlet temperature case, since the channel is long enough for the two curves to converge. Thus, uncertainty in the inlet temperature would probably not be a major cause of the elevated outlet temperature predicted by the model. The uncertainties in the parameters of specific heat and especially thermal conductivity are most likely the main contributors to the error in the prediction. This high prediction may also be attributed to the Nusselt number value of 3.66 which was used. This is the lowest possible value for the Nusselt number, and will yield the most conservative results.

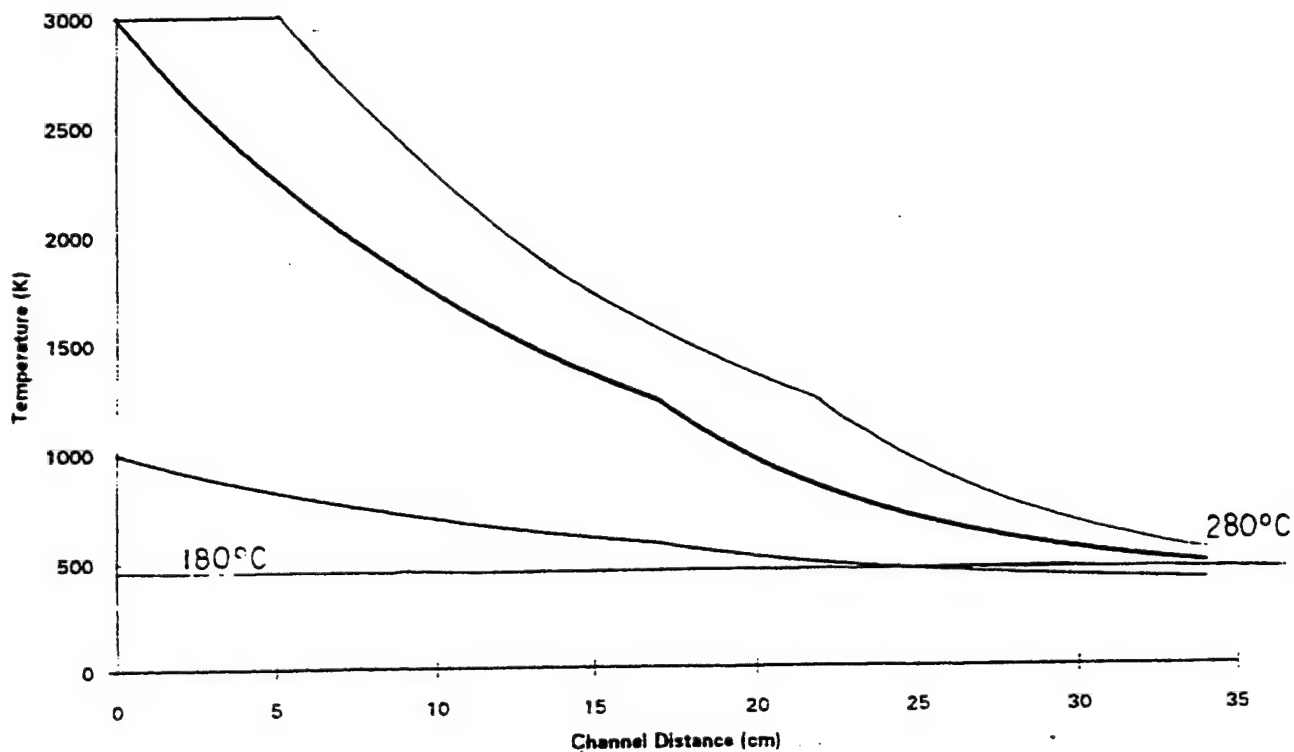


Figure 6. Theoretical Performance Curve for MWCD Model

In view of the geometry of the actual multichannel device and the violent and unsteady nature of the burning SFE it is expected that some turbulence in the flow is induced. This would increase the effectiveness of the heat transfer by increasing the convection coefficient and possibly explain the observed cooling.

#### b) Bunsen Experiments

Since the model of the multichannel device did not account for induced turbulence and since the uncertainty in the parameters was so large, it was desired to perform a test where the parameters were known to be more accurate, and where flow was known to be laminar, so that the accuracy of the model could be evaluated. For this experiment, a jet burner was used to simulate the flow of the hot SFE exhaust. The burner was chosen so that continuous, steady, temperature measurements could be made over a long period of time, and the experiment could be repeated to check for consistency. The burner was sealed to the flow chamber so that all of the exhaust gases are forced to flow through the ceramic channel. The ceramic tube used in this experiment was approximately 34 cm long, of rectangular cross section with dimensions 1 cm x 1.9 cm. This geometry yields a hydraulic diameter  $D_h = 1.31$  cm. Thermocouples were placed at the inlet and outlet of the ceramic tube. These thermocouple probes were connected to a scanning thermocouple thermometer

which read the temperatures at the probe locations every ten seconds. Flow meters were used to set the flow rates of the natural gas and air which entered the burner to achieve the desired flame. An additional air supply was needed to stabilize the flame after it was inserted into the sealed compartment, and an additional flow meter was used to set the supplemental air flow. The flow meters were calibrated with a bubble meter, and the volume flow rates were converted to mass flow rates based on the density of the gas. The total mass flow rate through the ceramic channel was set at about 0.22 g/s ( $2.2 \times 10^{-4}$  kg/s) and held constant through the duration of the experiment. (For an SFE charge of 500g which burns in 100 seconds, about 23 channels would be necessary to achieve a similar flow rate.) Figure 7 is a plot of the thermocouple readings as a function of time for the first ten minutes of the experiment. The plot of Figure 7 shows that the system reached a steady state condition about 1 minute after the exhaust was introduced to the channel which remained steady for about 3 minutes thereafter. During the 3 minute period the inlet temperature remained fairly constant at about 900K and the outlet temperature was fairly constant at about 520K.

For analysis using the model, it was assumed that the exhaust was air and the properties were approximated as being those of air at the average temperature between the inlet and the outlet. At an average temperature of about 750K,  $C_p(\text{air}) = 1087 \text{ J/kgK}$ ,  $k(\text{air}) = 0.0549 \text{ W/mK}$ , and  $\mu(\text{air}) = 354.6 \times 10^{-7} \text{ Ns/m}^2$ . Based on the mass flow rate, viscosity and hydraulic diameter, the Reynolds number was calculated to be about 592 (laminar), which indicates that a Nusselt number of 3.66 is appropriate. The convection coefficient was then calculated to be approximately  $15.3 \text{ W/m}^2\text{K}$ . With these parameter values and an inlet temperature of 900K, the model predicted an outlet temperature of 523K at the exit of the ceramic tube (See Figure 8), which matches the experimentally obtained values of 520K almost exactly.

The model provided very accurate results for the steady, laminar flow burner experiment where air is the fluid medium. It is expected that the model will also work well for flows which are in the turbulent regime. As demonstrated by the multichannel ceramic case, the model does not account for turbulence which may be induced by the geometry of the device or unsteady burn rates. Also the uncertainty in the values for the parameters of specific heat and thermal conductivity may result in conservative results. In reality, the exhaust probably had a higher conductivity and the flow was more turbulent than what was assumed by the model. To achieve more accurate results with the model, it is necessary to obtain accurate values for the physical properties of the SFE exhaust stream, and to have better knowledge of the flow characteristics. The following section is devoted to the use of the model in determining an optimum configuration for a 500g device.

## 5. Optimizing Ceramic Channel Configurations

The first step in optimizing a flow configuration is to select the optimal channel geometry. It is desired to obtain the maximum exposed perimeter area (PA) for a given cross sectional flow area (FA). This ratio PA/FA is increased as the channel cross sections are made longer and thinner, reaching a maximum at an infinitely long and infinitely thin cross section. Not only is this configuration impossible, but extremes in this direction would provide too much resistance to flow and generate a large pressure build-up at the combustion zone. Thus, to avoid such a scenario, the smallest dimension of any channel will be limited to 0.5cm. As a practical example, a 6cm x 0.5cm cross section will be analyzed. Thus, the flow area

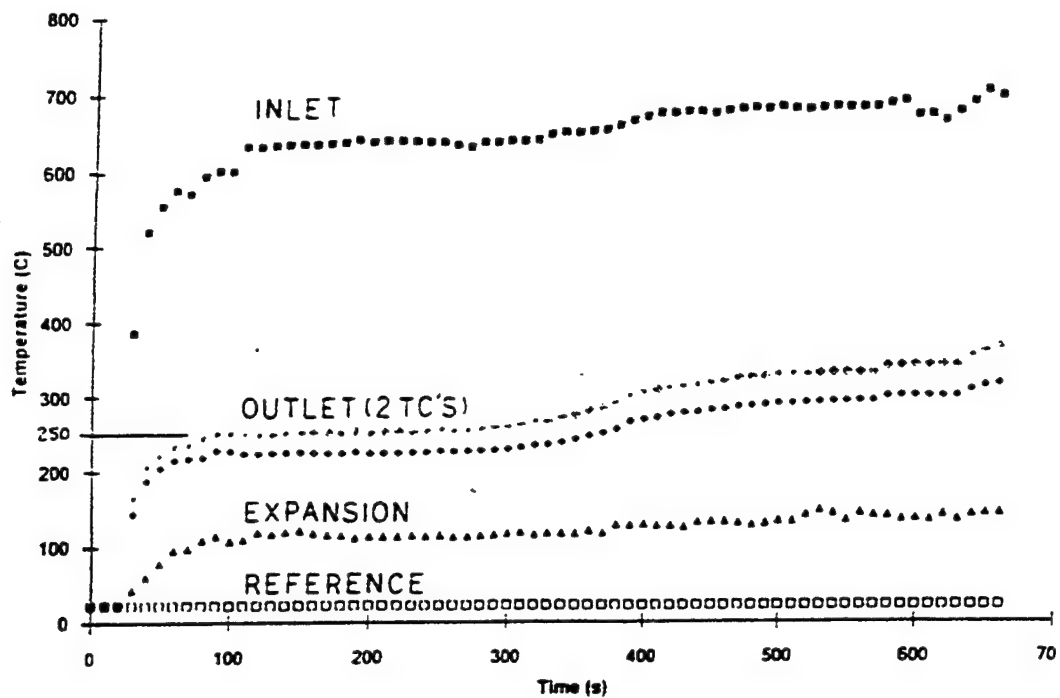


Figure 7: Thermocouple Data From Bunsen Experiment

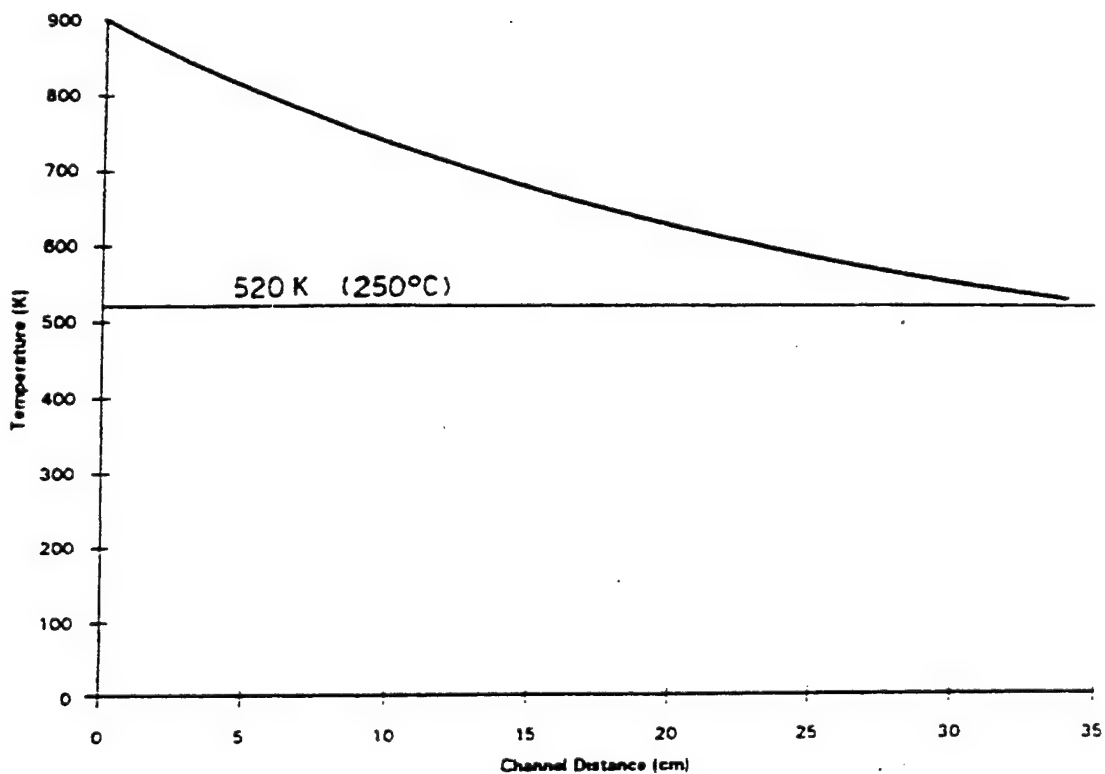


Figure 8: Theoretical Performance Curve for Bunsen Model



according to our restrictions, a 6cm x 0.5cm cross section is optimal, and this is the channel which will be analyzed. The flow area per channel is  $3\text{cm}^2$  and the 'wetted' perimeter is 13cm, yielding a hydraulic diameter,  $D_h = 0.92\text{cm}$ . The next step is to determine the number of channels which would provide optimal cooling based on the approximate 5g/s burn rate. A smaller number of channels will cause the flow to be more turbulent through each channel, thus increasing the convection coefficient; however, the residence time will be decreased with an increase in velocity, reducing the amount of time for heat transfer to take place. A smaller number of channels will also result in less total surface area for heat transfer to take place. Thus it is expected that the optimum configuration will be the one which utilizes the most channels with the flow still being in the turbulent regime.

For the 6cm X 0.5cm channels, and a 5g/s total flow rate, an analysis has shown that the cooling effectiveness increases with increase in channels up to seven channels where the Reynolds number is about 2800. This number is fairly close to the critical Reynolds number of 2300 where the flow has the potential of turning laminar. Due to the uncertainties in the parameters used in this analysis, it will be assumed that the seven channel device provides the optimum configuration. It should be noted that this result relies heavily on the value used for fluid viscosity and burn rate. If the viscosity or burn rate is much different than that which was approximated, the optimum configuration may not be seven channels.

The remaining dimensions to be specified are the ceramic wall thickness and the channel length. Since heat transfer occurs only at the surface of the ceramic wall, excessively thick walls will not enhance the cooling capability of the device. An average wall thickness per channel of about 3mm should suffice. Assuming that the channels stay wet throughout the burn, a channel length of 20 cm would result in an outlet temperature of about 230C based on the physical parameters used in the MWCD analysis. It is expected that this value is high since the results from the MWCD analysis suggest that the value used for thermal conductivity was low. However, the assumption that the ceramic remains wet is not valid. In our experimental results with the MWCD and the ceramic tube, we have observed dry-out in the sections of the ceramic near the inlet where the temperatures were highest. In order to cool the exhaust of a 500g charge to 300C, the device would need to evaporate 700g of water. A seven channel device which is 20cm long, and assuming that heat could transfer effectively through a 3mm thickness of the ceramic, the device could only contain 311g of water to potentially cool the exhaust. Thus, much of the ceramic would dry-out and become ineffective, resulting in an increased outlet temperature. The only solution to this dilemma would be to either increase the channel length to compensate for the dry-out ( i.e. MWCD), or to provide a mechanism for continuously replenishing the ceramic (i.e. a pressurized reservoir which feeds the drying ceramic). In either case the device would have to be made considerably larger than what would contain a 7 channel, 20cm long ceramic cylinder with 3mm wall thickness per channel. In our original MWCD, assuming laminar flow, the heat transfer effectiveness of this device was somewhat less than half of the optimal design. However, efforts to reduce the size of this device would be constrained by the need to contain at least 700g of water which can readily be vaporized. Therefore, we have concluded that to sufficiently cool a 500g charge would require a device which is larger and heavier than that which could be considered easily throw able; however, such a device could serve as an effective stationary extinguishment generator.

## SECTION IV

### MULTICHANNEL FIRE TUBE BOILER

#### A. AUTOMOTIVE HEAT EXCHANGERS

Following our philosophy of building or adapting simple prototype devices in a search for promising arrangements for cooling SFE generated aerosols and baffling the flames we have built and tested one fifth to full scale devices incorporating car heater and car air conditioning type radiator-heat exchangers. These are already highly engineered for compactness, light weight and high efficiency and thus represent an excellent point of departure for adaptation to this particular cooling problem.

In the first 100 gram test with automotive type radiator the flame directly impacted the surface of an aluminum finned radiator and melted some of the tubes. In our subsequent tests the SFE charge was burned in an insulated chamber with a labyrinth arrangement for the exhaust smoke and gases, that finally passed through a heater type radiator filled with 300 ml of water. When a 100 gram pellet was tested, the smoke was cooled to 50 °C. With 200 grams of SFE the smoke was cooled to 80 °C. The next experiment was with 400 grams of SFE, which proved to be too much for that particular configuration. The radiator overheated and did not cool the smoke sufficiently. However, a radiator type heat exchanger appears to be a promising component of the solution to the 500 gram SFE problem.

In our most successful test of the radiator - heat exchange type of system we achieved in a 200 gram firing a cool smoke that had little tendency to rise. The "football grenade" system sketched in our November progress report was a conceptual extension of our 3rd radiator system that projected to be able to handle the 2400 BTU released by a 500 gram SFE charge. This system would take advantage of the following cooling mechanisms. 1) Heat Absorption (HA) by a HA substance or dissociating substance upon flame impact, 2) heat transfer to metal in passageways, 3) cooling by heat exchange with the metal and water in the tubes of the cylindrical heat exchanger (radiator) and 4) boil-off of water in pressure relief openings of the radiator tubes. The system would be thrown like a football into an opening in a flaming structure.

In most automotive radiator systems air to be heated or cooled passes through multifinned aluminum structures connected to water or liquid coolant bearing tubes that absorb or deliver heat to the gases passing through the fins. In some heat exchangers such as a fire tube boiler the hot gases are channeled in metal tubes embedded in water for the rapid production of steam.

A miniature 2 or 3-pass fire tube type boiler that separates the SFE aerosols and the steam generated in cooling could serve as a realization of the multichannel radiator heat exchanger approach. In this effort we are using an automotive air conditioning type heat exchanger as an initial component to insure light weight and high heat transfer rates needed in a throwable unit. The heat transfer in a single tube of a fire tube boiler is amenable to mathematical analysis [19] as given in the following section.



## B. FIRE TUBE BOILER ANALYSIS

### 1. Introduction

A major drawback to the ceramic channel design was the propensity of the ceramic to dry out, which requires either the channels to be made long enough to account for dry out, or a mechanism to replenish the drying ceramic with water. In a fire-tube type device however, a thin, highly conductive tube separates the hot exhaust from a bath of water. As water boils off the surface of the tube, cool water immediately replaces it. Thus, a device such as this could be much smaller in size than a comparable ceramic device. The following analysis is a summary of the effort made to evaluate the potential of a fire-tube type mechanism to cool the exhaust of a 500g charge which would be used in a throwable SFE canister. In such a device the exhaust from the burning SFE would pass through an array of highly conductive thin walled tubes which are surrounded by a bath of water. The hot exhaust would exchange heat with the water through the tube wall, causing the temperature of the exhaust to decrease as the water absorbs heat and changes phase.

### 2. Modeling the Fire Tube

The symbols introduced in Section III C are again used in this analysis. We here also introduce the additional symbol  $D$  = Nominal Tube Diameter. We assume that for thin walled tubes that under steady state conditions the wall temperature of the tube is relatively uniform and constant at 375K. With this assumption the model follows that of the ceramic channel very closely. Figure 9 illustrates a single fire tube with the aerosol exhaust as the internal fluid, and water as the external fluid.  $T_{m,i}$  is the inlet temperature of the exhaust,  $T_{m,o}$  is the exit temperature of the exhaust, and  $T_b$  is the bulk temperature of the water,  $d_1$  is the inner diameter of the tube,  $d_2$  is the outer diameter of the tube, and  $L$  is the length of the tube. Since the tube wall is assumed to be very thin, we refer from here on only to the nominal diameter,  $D$ . The model is based on the transfer of the thermal energy of the exhaust to the water bath which surrounds the tubes. As in the ceramic channel study, this model divides the tube into thin slices (perpendicular to the axis of the tube), where the gases in a slice move incrementally from one slice to the next. During steady state each slice was assumed to be isothermal. Using Eqs. 1 and 2 of our ceramics analysis it is first necessary to obtain values for the parameters  $h$ ,  $A_p$ ,  $m$ , and  $C_p$ . With these values, and an assumed inlet temperature (3000K), a temperature vs. tube length plot can be attained. The values for  $h$  and  $A_p$  rely on the size and number of tubes. Our experiments have revealed that for firings of 200+ grams of SFE type A powder, the burn rates are approximately 5g/s. It should be noted, however, that this value is partially dependent on the geometry of the fuel cell. For example, a longer, thinner fuel cell would yield longer burn times than a shorter, fatter fuel cell. The value for  $C_p$  will be the same as that assumed in the ceramic analysis as 1150 J/kgK.

In order to maximize the effectiveness of the heat transfer, it is desirable to have turbulent flow through the tube, with a long residence time. However, for a given tube, an increase in turbulence would require an increase in velocity, which would decrease the residence time. Thus, it would be desirable to achieve a flow which was near but greater than the critical Reynolds number of 2300 where the flows typically transition from laminar to

turbulent. In this analysis we will assume an optimal Reynolds number of 3000 to accommodate for uncertainties in the physical parameters of the exhaust. If the viscosity of the exhaust is approximated as that of air at an average temperature of 1700K (as in the ceramic study,  $\mu = 370 \times 10^{-7} \text{Ns/m}^2$ ), the equation for Reynolds number  $Re = 4m/\pi D \mu = 3000$  can be used to determine the optimal tube size and number of tubes. Rearranging this equation in terms of D yields  $D = 4m/3000\pi\mu$ . In this equation, m is equal to 5g/s divided by the number of tubes. Thus, the optimal diameter is approximately  $5.7/(\text{\#tubes})$  cm. Thus, for example, an optimum configuration would be 10 tubes of 0.57cm diameter. It can be shown that theoretical performance improves as the number of tubes increases with decrease in tube diameter, however we will limit the minimum diameter to 0.57 cm to prevent excessive pressure build-up. It should be noted that this 'optimal' configuration relies on the value chosen for viscosity, which is unknown for the exhaust stream but which is probably higher than that of air due to the presence of solid particulates. Therefore, the optimal geometry may require fewer and/or smaller tubes.

Assuming that the flow is in the turbulent regime, the Nusselt number can be determined from the correlation  $Nu = hD/k = 0.023Re^{0.8}Pr^{0.3}$ . Assuming a Prandtl number of about 0.7 and a thermal conductivity  $k=0.12\text{W/mK}$  (consistent with the ceramic study),  $Nu = 12.5$ , and the convective heat transfer coefficient for the exhaust flowing through a tube is about  $263\text{W/m}^2\text{K}$ . Using this value along with m and  $A_p$  for a single tube will yield a temperature vs. distance plot along the length of a tube in the device. Figure 10 is a plot of temperature vs. tube length for two fire tube devices. The upper curve in the figure is for a device which has 10 tubes of 0.57cm diameter. As shown in the figure, a device with tubes of 31.5cm length would reduce the exhaust temperature down to about 300C. Based on the results of the ceramic study analysis of the MWCD, the approximate value for thermal conductivity of  $0.12\text{W/mK}$  may be low, resulting in conservative predictions by the model.

The equation for the upper curve in Figure 10 for a device using round tubes and the parameters given was  $T_{n+1} = T_n - 0.0082(T_n - 375)$ . If we were to use tubes of longer, thinner cross section while keeping the Reynolds number per tube the same (approx. 3000), we would expect improved cooling effectiveness due to the increased area for heat transfer. For example, a device with seven 0.5cm x 6cm channels (as was the 'optimum' configuration in the ceramic study), having a hydraulic diameter  $D_h = 0.92\text{cm}$ , would result in a Reynolds number of about 2815. A device with these dimensions would yield a temperature vs. length equation that becomes  $T_{n+1} = T_n - 0.024(T_n - 375)$ . The lower curve in Figure 10 shows the temperature vs. length performance for the new device. As seen in the plot, the outlet temperature now reaches 300C in only 10.7cm length of tube. A comparison of the two curves demonstrates how the perimeter to cross-sectional area ratio of a flow channel has significant influence on the effectiveness of the device to transfer heat. The predicted performance of this device is actually identical to that of the 'optimal' ceramic device (continuously replenished) of the previous section, since all parameters are identical. Thus the model predicts that the size of an effective 500g device can be considerably smaller than a one gallon can but the device will not be much reduced in weight due to the requirement for a large amount of water to absorb the heat released by the SFE.

### 3. Experimentation

Experiments were set up to assess the potential of a realistic device. In our early experiments, however, it was noticed that the aerosol particles would adhere to the inner wall of the tube, creating an insulative layer of the particulates between the metal tube and the hot exhaust. This behavior has two major drawbacks: 1) It robs the exhaust stream of its fire fighting components, thereby reducing its effectiveness as an extinguishant, and 2) It severely diminishes the cooling performance of the fire tube device. Although this device would be ideal for a purely gaseous stream, to cool the SFE exhaust it is necessary to find a suitable material for the tube or for a lining of the tube which does not exhibit this adhesive behavior. Although one might expect otherwise, this adhesive behavior was not observed in our wet ceramic experiments. To cool a 500 gram SFE charge in a throwable device, a fire tube type canister holds the most promise, providing that a method can be devised with which the exhaust can pass cleanly through the device.

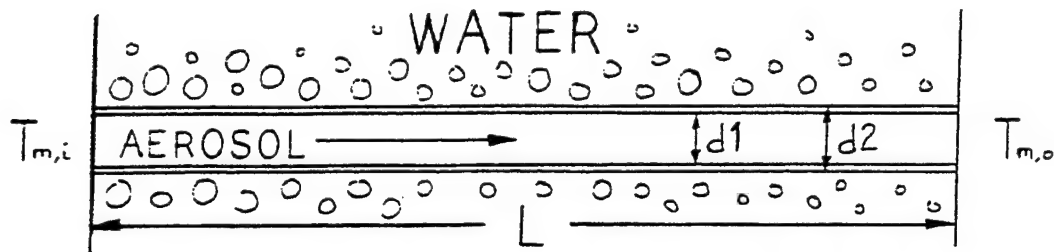


Figure 9: Schematic Diagram of a Fire Tube

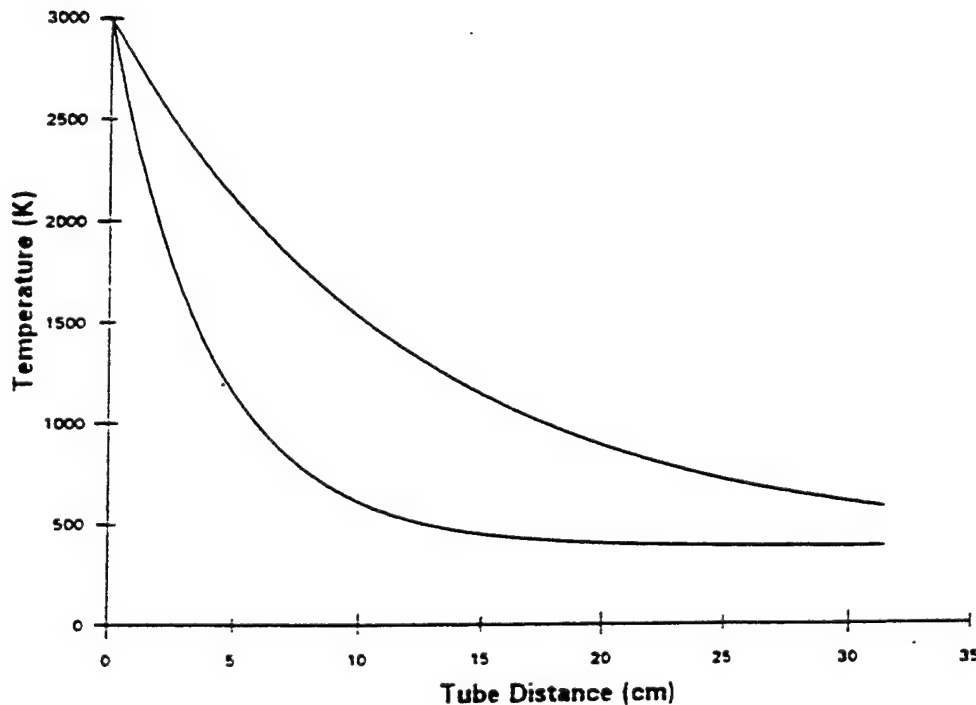


Figure 10: Theoretical Performance Curves for 'Optimal' Fire Tube Devices

## SECTION V

### HEAT RETENTION AND RADIATION DEVICES

#### A. CARBONATE HEAT RETENTION DEVICES (CHRD)

Because the SFE material releases such a large amount of heat, many difficulties have been encountered in cooling the container and the aerosol exhaust to acceptably low temperatures. One possible way to reduce the size of a device which contains a suitable amount of the SFE material so that it may be considered throwable would be to provide a heat sink directly at the combustion zone. Table 3 in Section II lists the dissociation temperatures of ceramic materials that might be mixed with powdered SFE to absorb part of the combustion energy. Table 4 lists the heat absorbed in raising selected materials to intermediate temperatures.

SPECTREX has reported that cooling directly at the combustion zone may lead to extended burn times and incomplete combustion. Rather than dismiss the heat absorption approach experiments were carried out to determine whether the benefits of cooling at the combustion zone would outweigh the possible adverse effects. Experiments were performed using dolomite powder, blended in with the SFE powder. Dolomite ( $\text{CaMg}(\text{CO}_3)_2$ ) dissociates at high temperatures, via the reaction:



This process absorbs about 1.54 kJ/gram of dolomite, based on calculations performed using heats of formation [20,21]. Assuming that the SFE material releases 2200 BTU/lb (SFE A and B), or 5.1 kJ/gram, burning 200 grams of SFE would release 1.02 MJ of energy. Thus, 660 grams of dolomite could potentially absorb the same amount of energy released from 200 grams of SFE. Table 5 lists the experimental results we obtained using dolomite blends.

Carbon dioxide gas, a product of the dissociation of dolomite, is a commonly used fire extinguishant as it displaces oxygen and "smothers" the fire. Therefore, the use of dolomite as a cooling and heat retention mechanism provides the fringe benefit of additional extinguishing capability. Each gram of dolomite could yield 0.477 grams of  $\text{CO}_2$  based on the molecular weights of the atoms and .523 grams of  $\text{CaO}$  and  $\text{MgO}$ . It might be noted that the residue left, where the SFE- dolomite blend originally was, glowed red hot long after the burn indicating substantial heat retention, the primary benefit of this cooling approach.

Prior to running the experiments, it was assumed that increasing the amount of dolomite would increase the burn time, until the combustion process was no longer self sustaining. Since dolomite is a blend of calcium carbonate and magnesium carbonate, which are both common minerals, the potential for each of these individual substances was explored. Calcium carbonate (limestone) will absorb 1839 J/g upon dissociating, and will yield 0.44g of  $\text{CO}_2$  per gram of  $\text{CaCO}_3$  [[20,21]. Magnesium carbonate will absorb 1191 J/g upon dissociating, and will yield 0.52g of  $\text{CO}_2$  per gram of  $\text{CaCO}_3$ . Thus for a given amount of heat absorption, one would require less mass of the calcium carbonate. If, however, the same heat absorption could be achieved with the magnesium carbonate, the  $\text{MgCO}_3$  would release more carbon dioxide and probably faster since the dissociation occurs at lower temperature.

Table 4. Heat Absorption by Selected Materials

Material	<- Heat absorbed by heating to->		Temp. required for for dissociation or phase change
	BTU/lb	<sup>o</sup> F	
Water	1685	1200 <sup>o</sup>	212 <sup>o</sup>
Boric Acid * $B_2O_3 \cdot 3H_2O$	1175	1200	starts 400 <sup>o</sup> F
10 Mol Borax * $Na_2 \cdot 2B_2O_3 \cdot 10H_2O$	1220	1382	
Limestone 1) $CaCO_3$	1160	1440	1440
Koalin Clay 1) $Al_2O_3 \cdot 2SiO_2 \cdot 2H_2O$	534	1200 <sup>o</sup>	1060 <sup>o</sup>

\* Private communication from U.S. Borax

1) The specific heat of both Limestone and clay are about 0.23 BTU/#/<sup>o</sup>F.

Table 5. Experimental Results Using Dolomite Blends

Fuel Mass (g)	Dolomite Mass (g)	Fuel Can Diam. (in.)	Burn Time (s)	Complete Combustion?	Exhaust Temp. (F)
100	0	2.25"	28	Yes	1765
100	25	3"	24	Yes	-----
100	54	3"	62	Yes	792
100	100	3"	85	No	911

## B. RADIATIVE COOLED AND BAFFLED DEVICE (RCBD)

The requirement for cooling the aerosols and gases from an SFE burn could be reduced significantly if the radiation from the combustion zone escaped the device. If physically possible this might reduce the remaining cooling problem by about 50 %. In pursuing this concept we attempted to get an independent estimate of the burn temperature by the novel spectroscopic method described in Section 2B. Basically we measured the spectrum of the SFE flame as observed with out 1200 l/mm grating with our computer spectrograph system through a nickel sulfate filter. This spectrum was compared with the spectrum of a tungsten halogen lamp carrying standard 8 amperes current that should have a temperature of about 3000K. The fact that the peak shifts to shorter wave lengths as the current and hence temperature increases supports this type of measurement. Measurements with pool fires with relatively low temperatures of about 1500°K indicate radiation heat losses of the order 40%. The Stefan Boltzmann Law ( $R=\sigma T^4$ ) [22] suggests that the radiative heat losses might in this case exceed 50% if it can escape the device.

The practical utilization of this approach is dependent upon whether it is possible to fabricate a device that will let the radiation but not the flames escape and which will redirect the aerosols and lower their temperature. While this requires a very difficult combination to have in a throwable device it may not be physically impossible. We have tested two potential partial realizations of this concept in the form of soccer ball sized devices weighted so that the radiation would escape upward. Figure 11 is a sketch of such a device. The shaded zone represents a region that should pass most of the high temperature radiation. At the same time the surface skin should redirect the flame and aerosols so that the flame is retained and the aerosols are cooled. Mica may be a potentially practical covering that could perform this function. It is used in wood stoves to allow heat to escape into a room while the hot gases and flame is redirected up the chimney. This is an analog of the present need. It might also be noted that Martin Marietta is developing a industrial diamond film depositing technique that might be adapted for this purpose.

We have been concerned that even if the radiation initially escapes the mica windows would be quickly coated by particulates. However the tangential redirection of the flow might minimize deposition during a short burn time. Fabricating a spherical shell of mica or industrial diamond appears beyond immediate realization. However, using a wire grid in which flat mica or diamond surfaces cover the wire openings should be within the realm of feasibility, albeit a difficult fabrication problem.

In May 1995 we secured some mica sheets that would have enabled us to construct a crude model of a device intended to take advantage of radiative heat loss. However by then, lacking a definition of "throwability", we were attempting to complete our single channel studies, theoretical modeling and flame suppression mechanisms studies.

## C. THROWABILITY OF SFE DEVICES

The problem of cooling SFE type aerosols has already been addressed in stationary devices that do not have severe weight, size and shock limitations [18] of a "throwable" device. Whether the cooling and flame containment needed in practical systems has always been achieved in such devices is still an open question. To a large



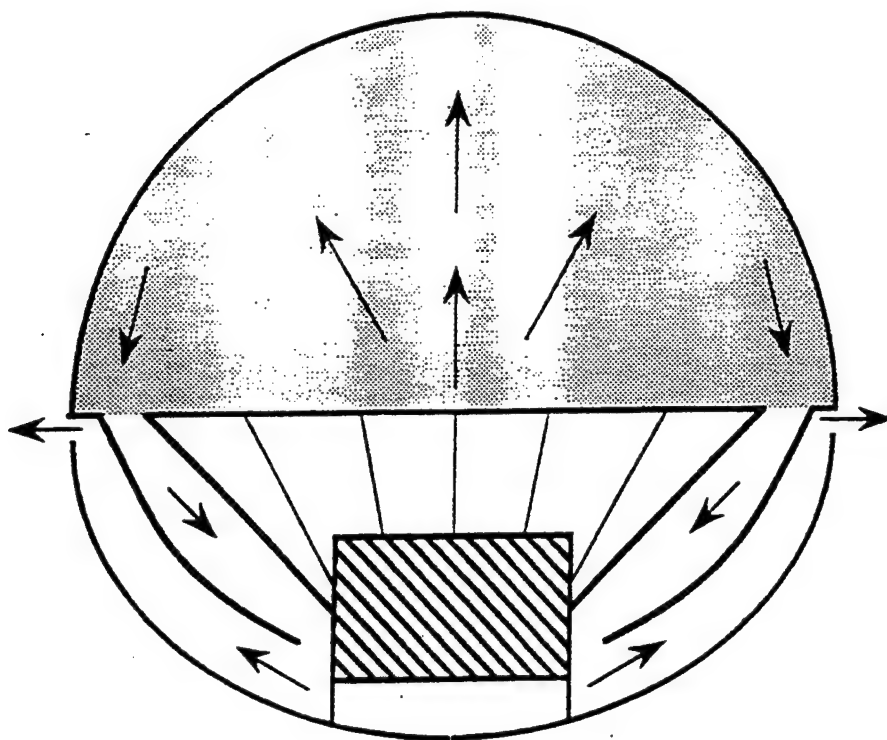


Figure 11. Radiatively Cooled and Baffled Device

extent the feasibility of developing a hand thrown SFE device depends upon the specifications of "hand thrown" or "throwability". We have sought clarification of this issue without success. We have also consulted with athletic capabilities experts in an attempt to find a scientific literature on this topic but could not find any quantitative publications. Accordingly we carried out some simple experiments within our group to get order of magnitude estimates.

Our tests indicated that throwing a 6 pound, gallon sized cannister into a 1 square yard opening 3 yards high at 5 yards range could be accomplished by a fireman in good physical condition about 90% of the time. The damage and distortion to this device did not seem beyond the capabilities of reasonable shock absorbing measures. If the device is hurled with a lacrosse type stick, longer ranges could be achieved. For still longer ranges a spring loaded or compressed air catapult might be used to reach a desired throw distance.

The throwable range increases materially if the weight and size limits were reduced say to 3 pounds and one half gallon. Then 10 or somewhat more yards would be a feasible range. Our experiments and analysis suggest it will be practically impossible to bring a device with a 500 gram SFE charge to such device weights and size limits, contain the flame and be shock resistant. One might accomplish the same overall objective by reducing the SFE charge to say 250 grams so as to be able to construct a lighter and smaller device and to throw two units. However the assignments of sub-tasks 3 and 4 of Task 3.08 were for 500 grams.



## SECTION VI

### MECHANISMS OF FLAME SUPPRESSION

#### A. FUNDAMENTALS

To place this work in perspective it is important to take a long range view of what we understand about the science and technology of fire. The uncontrolled initiation of fire goes back to the beginning of the earth's oxygenated atmosphere associated with the development of plant life, perhaps a billion years ago. The controlled use of fire, mankind's oldest technological achievement, goes back about one half million years as estimated by fire place datings to homo erectus (before homo sapiens!). Despite these ancient beginnings we still do not have a complete understanding of the fundamentals of combustion. Indeed many textbooks still use gross oversimplifications such as  $\text{H}_2 + \text{O}_2/2 \rightarrow \text{H}_2\text{O}$  to explain hydrogen combustion. Yet for many decades combustion scientists have known that this simple reaction proceeds through a chain of intermediate steps involving the OH, H and O and other free radicals.

As noted in the introduction (Section I C) the search for halon replacements has focused attention on the still unsettled issue of flame extinction mechanisms. The recent article in Chemical and Engineering News (C&EN) [1] that described European quests for halon alternatives brought several points that are particularly relevant to PGS programs. 1) The fundamental theory of flame suppression by halons is still very unsettled despite the use of halogen based extinguishers since 1907. 2) Thus far all gaseous substitutes are less effective than halon 1301. 3) Some progress has been made in gathering reaction rate data that might eventually help provide the basis for a kinetic theory of fire suppression when halogens are the active agent. 4) Lack of success with gaseous agents enhances the incentives to drive home an aerosol suppressant approach. 5) Particulates in the form of finely ground powders of selected chemicals have been used for fire suppression for over four decades. The most accepted theories as to their action invoke thermal mechanism. 6) In view of the large thermal heat release in proposed PGS devices cooling the pyrotechnically generated particulates or gases should be critical to their successful use as fire suppressants. 7) If free radical scavenging can play a major role the cooling, weight and size requirements should be more modest. 8) Clearly we would make more rapid progress in developing halon alternatives, particularly PGS systems, if the basic physical and chemical mechanisms involved in fire and fire suppression were better understood.

Among existing attempts to explain fire suppression the Thermal (TH) approach of Ewing et al.[2] correlates flame extinction by halons and particles with heat capacity and endothermic reaction sinks. On the other hand the Free Radical (FR) approach of Westbrook [3] invokes scavenging of OH, H and other free radicals to interrupt the important fire sustaining chain reactions. The fact that these contrasting approaches have still not been reconciled [1] is a sad commentary on fire suppression research over the decades.

The problem of suppressing fires by pyrotechnically generated suppressants (PGS) may be more difficult than the problems of initiating or maintaining fires. Thus it may be difficult with non-explosive pyrotechnic devices to: (1) remove heat,

(2) remove fuel, or (3) remove oxygen, the three classic methods of extinguishing fires. It has generally been assumed that the halons work by a 4th mechanism, breaking the chain reactions involved in the complex chemical reactions under way in fires. However some groups[1,2] claim that this has not been proven and that thermal mechanisms alone can explain halon action. It would appear that the main hope for success with PGSSs particularly SFEs, lies with chain breaking mechanisms since the catalytic nature of this mechanism permits a little extinguishment to multiply its effect. Indeed the stratospheric ozone depletion problem itself is serious because through cyclic reactions one chlorine or bromine atom can destroy thousands of stratospheric ozone molecules [23]. Since there is still controversy as to halon action, in the CCTL flame suppression studies we have focussed on the development of observational methods of measuring the decay of the OH and other free radicals when flames are subjected to halon and aerosol-type suppressants.

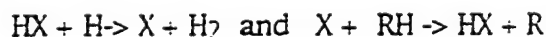
In the course of our exploratory spectroscopic studies under Task 3.06 several thermal extinguishment mechanisms not considered by others were encountered. These included (a) increased blackbody continuum radiation, (b) increased soot, and (c) increased CO production. The decreased combustion efficiency, due to increased carbon monoxide and soot production as well as the increased radiation are cooling mechanisms that could contribute to flame extinction. From our computer literature searches of the flame suppression literature since 1990 we could not find any citations indicating that these mechanisms have been considered in either TH or FR or any other approaches to the fundamentals of flame suppression mechanisms.

In examining previous fire suppressant studies we found practically no references to ultraviolet-visible (UVV) spectroscopy. This is puzzling since UVV spectroscopy has historically led to an understanding of the chemistry of flames, the development of some of the most sensitive chemical analysis techniques along with the quantum theory of light and of atomic and molecular structure. The fact that UVV spectroscopy when applied in our military and space program [4,22,23] led to the recognition and quantification of the stratospheric ozone depletion problem itself makes it doubly puzzling that this important analysis technology had been overlooked in halon replacement studies intended to protect the stratospheric ozone layer.

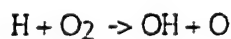
Multichannel ultraviolet visible spectroscopy (MUVV), can display the fate of fire-maintaining free radicals when reacting with suppressants. For example the interaction of halon suppressants  $\text{CF}_3\text{X}$  ( $\text{X}=\text{Cl}, \text{Br}, \text{or I}$ ) with hydrocarbons typically leads to the acid  $\text{HX}$ . A simplistic explanation of scavenging might be given by assuming that these acids depletes OH radicals through reaction cycles such as



A more complex explanation might be given by the reaction cycle used by Glassman [24] in explaining soot nucleation



where R is any hydrocarbon molecule. The scavenging of H radicals via this catalytic cycle enhances soot nucleation. The fact that it also reduces the production of OH and O radicals that would otherwise be formed by the reaction



impedes the normal fire chemistry.

## B PROPANE FLAME-SUPPRESSANT INTERACTIONS

Both explanations of free radical scavenging described above reinforced our initial judgement [4,12,23] to focus on OH observations by the use of middle ultraviolet emission spectroscopy. In our exploratory spectroscopic survey we used a system consisting of an 1/8 meter crossed Czerny-Turner spectrograph (Oriel MultiSpec 125) with 400 1/mm and 1200 1/mm gratings. The detection system consist of a 1024x256 pixel (Oriel 77174) Charge Coupled device (CCD) feeding into a 80486 level personal computer. We used a propane flame as a convenient gaseous fuel with a hydrogen/carbon atomic ratio (8/3) not very far from typical oil fuels (H/C ~ 2).

We reasoned that the reduction of OH and other free radicals emission could provide data useful in building a model of suppressant action on representative pool fires and in selecting the most efficient aerosol fire suppressants. In addition many species not active in the IR are active in the ultraviolet-visible region and could be measured by on line middle ultraviolet spectroscopy (MUV). While many fire suppressant stuies make use of infrared observations most of the infrared radiance associated with a flame comes from post-reaction zone products. In contrast reaction zone processes are frequently dominant in the ultraviolet.

Figure 12 is a synthesis of several exploratory spectra taken of a propane flame with 1211 suppressant using the 400 1/mm grating. These spectra taken in connection with our work on Task 3.06. is illustrative of the potential information content of MUVV spectra of flames. The spikes at 590 nm and 760 nm are probably from sodium and potassium contamination of our system by SFE firings. The increasing Planck continua above 500 nm as halon levels increase is suggestive that enhanced radiation with suppressant injection may be a contributing factor in the action of halons and possibly other fire suppressants.

Figure 13, a computer generated enlargement of the OH emission region near 300 nm in Fig. 12 indicates that increasing halon suppressant levels is associated with decreasing OH emissions. While many theoretical works have called attention to free radical loss due to halons we were unaware of prior direct observational displays of this mechanism. Unfortunately through an error of calibration the location of the OH radical emissions in Figure 13 appear near 300nm rather than 308nm. This necessitated new experiments in which the MUV spectra were taken directly with a UV grating, while halon concentrations were increased, with careful attention to wavelength calibration.

The main hope for success with small levels of pyrotechnic fire suppressants may, as was thought to be the case with halons, lie with catalytic breaking of the chain reactions involved in the complex chemical reactions under way in fires. These chains are largely propagated by free radicals such as OH, H, O, CH, etc. Accordingly, in connection with sub-task 3.08-2 we focused on measuring and modeling the decline of the OH and other free radicals when subjected to halon or aerosol-type suppressants.

In these efforts, flame spectra were generally taken without suppressants and then with the halon suppressants 1211 (CF<sub>2</sub>ClBr) and 1301 (CF<sub>3</sub>Br). With the 400 1/mm grating, one exposure covered the 250 to 800 nm spectral region (the UVV spectrum) we found that for yellow flames, and/or those which generate soot, the black body (Planck continuum) becomes dominant and molecular features become less apparent. However, using a 1200 1/mm grating, we could focus on the narrower MUV spectral region.

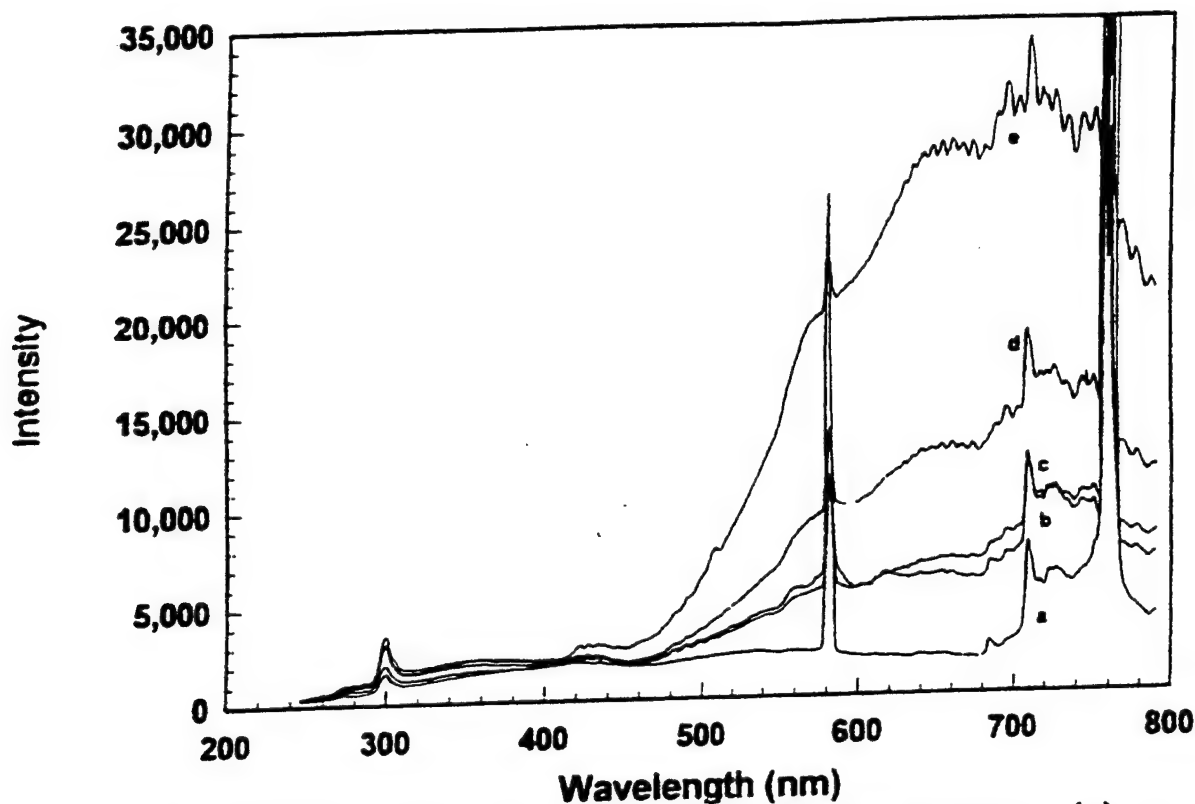


Figure 12. Methanol pool fire with halon 1211 suppressant : (a) no suppressant, (b) 1211 at 26 ml/min, (c) 1211 at 40 ml/min, (d) 1211 at 60 ml/min, (e) 1211 at 128 ml/min.

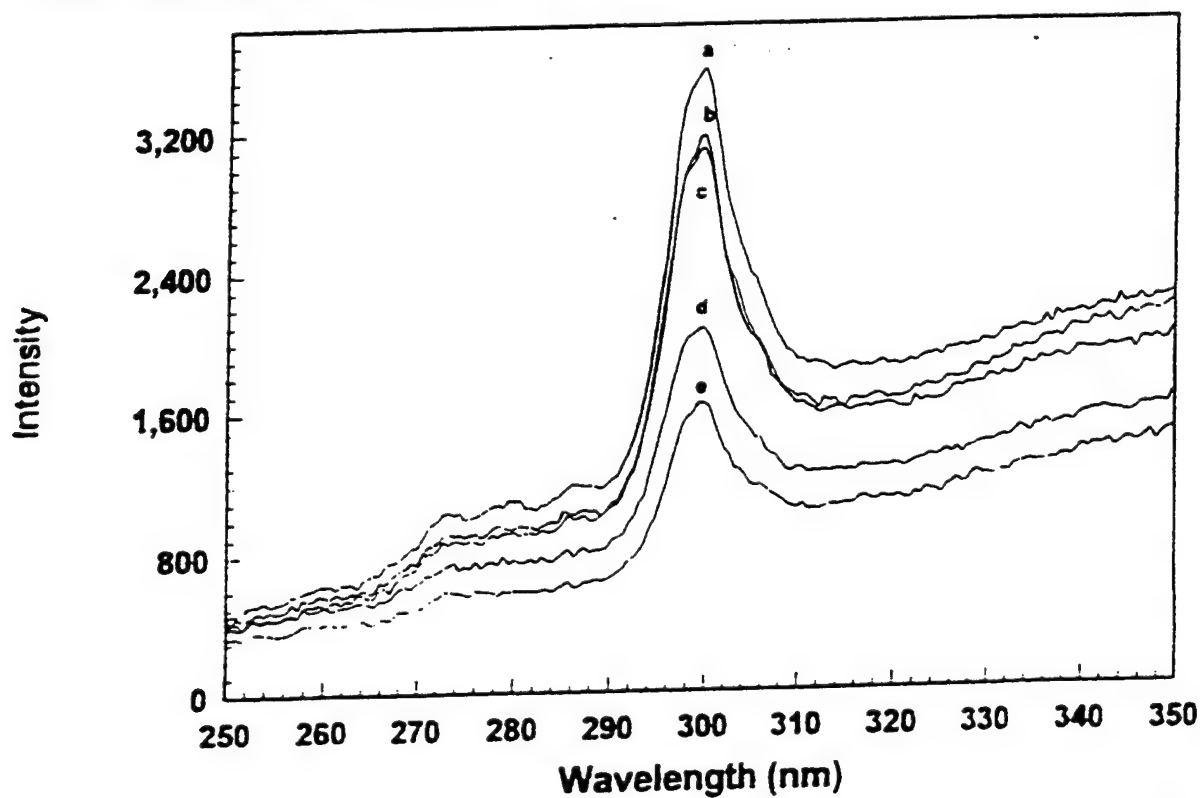


Figure 13. Methanol pool fire with halon 1211 suppressant (OH region). Notice the reversal of trend: (a) no suppressant, (b) 1211 at 26 ml/min, (c) 1211 at 40 ml/min, (d) 1211 at 60 ml/min, (e) 1211 at 128 ml/min.

### C. STRAY LIGHT REJECTION

Since the short wavelength fall-off of the Planck radiation is very precipitous we concluded that Planck radiation need not overwhelm the 308 nm region OH emissions if precautions are taken with respect to stray visible and near infrared light. In our Applied Optics Technote [10] we illustrated the stray light problem and the solution with the spectra of propane diffusion flames injected with halon 1211. We concluded that by minimizing stray light that it should be possible to "see" the emissions of OH, the major free radical operative in hydrocarbon flames even in the case of smokey fires. By using stray light rejection techniques used in solar ultra violet spectral measurements [25,26] the MUV could be used to gain information useful to the understanding of flame suppressant mechanisms.

Halon replacement studies in response to the Montreal Protocol have made practically no use of middle ultraviolet (MUV) spectroscopy. The oversight appears to have arisen because fires are usually smoky and generate such large black body continua that free radical and molecular emissions are generally overwhelmed. However, by suitable attention to stray light rejection techniques it is possible to observe free radical emissions in the 200-400 nm region and obtain valuable information on suppressants-flame interactions.

The MUV radiation from flames is strongly influenced by free radical mediated non-equilibrium processes which characterize irreversible combustion reactions (and chemiluminescence). For hydrogen containing fuels the hydroxyl (OH) radical is usually the chief radiative species giving rise to a series of strong bands in the 281 to 325 nm range. The intensities of the OH bands are sensitive to the flame system, reactant type, impurities, pressure and other experimental variables and hence can convey useful information on flame processes. The infrared spectral region, while useful in showing the final products of combustion conveys little information on combustion chemistry or processes.

In sooty luminous flames the Planck continuum in the visible and infrared (VIR) usually overwhelms molecular features. The addition of halon suppressants creates extra soot thereby enhancing black body radiation at least until extinguishment levels are reached. However, calculations using Planck's function show that this continuum should be very small shortward of 400 nm in the 800-1600 K temperature range typical of sooty fires. Unfortunately, imperfections in the optics of most spectrometers often lead to contamination of the middle ultraviolet channels by stray VIR light. In our program we reduce stray light by borrowing from techniques used in measurements of solar UV radiation reaching the ground that were motivated by the stratospheric ozone depletion problem itself [26,27]

We illustrate the efficacy of stray light rejection measures with our computer spectrograph system using a propane diffusion flame in which a moderate amount of halon agent is added to the fuel upstream of the linear burner. The visible-ultraviolet spectra (250-800 nm) obtained with a 400 line /mm grating is practically devoid of molecular features and has a very large peak in the 700-800 nm region that increases with halon additions due to enhanced soot formation.

Using a 1200 l/mm grating blazed and centered for 300 nm we obtained the spectrum labeled A in Figure 14. The 306-309 OH features and other possible weak molecular features are observable, however, stray VIR light dominates the spectrum. Measures to mitigate stray light problem include: (1) using quartz or fused silica based short or band pass filters that pass MUV light but absorb VIR light with a

tolerable leakage, (2) eliminating the zeroth order spectrum by placing black felt on areas of reflection inside the spectrograph, (3) conical baffling of the internal entrance and exit zones of the spectrograph to avoid overfilling the mirrors and grating and (4) externally covering of the spectrograph with black felt, and (5) additional retrofit measures taken by Oriel involving the use of felt and light traps inside the spectrograph. Figure 14B shows the MUV spectrum, with tentative molecular identifications, of a similar flame after spectrographic improvements were made and a solar blind filter used (Corion Corp. Filter No. SB-300F). Not only are OH emissions much more distinct but products of flame-suppressant interactions (CCl and CBr) are also observable. The compounds  $C_6H_6$  (benzene),  $CH_2O$  (formaldehyde), and CHO were probably formed in the diffusion flame under substoichiometric soot generating conditions. Additional MUV spectra taken at higher halon injection levels are similar to Fig. 14B but with lower OH emissions.

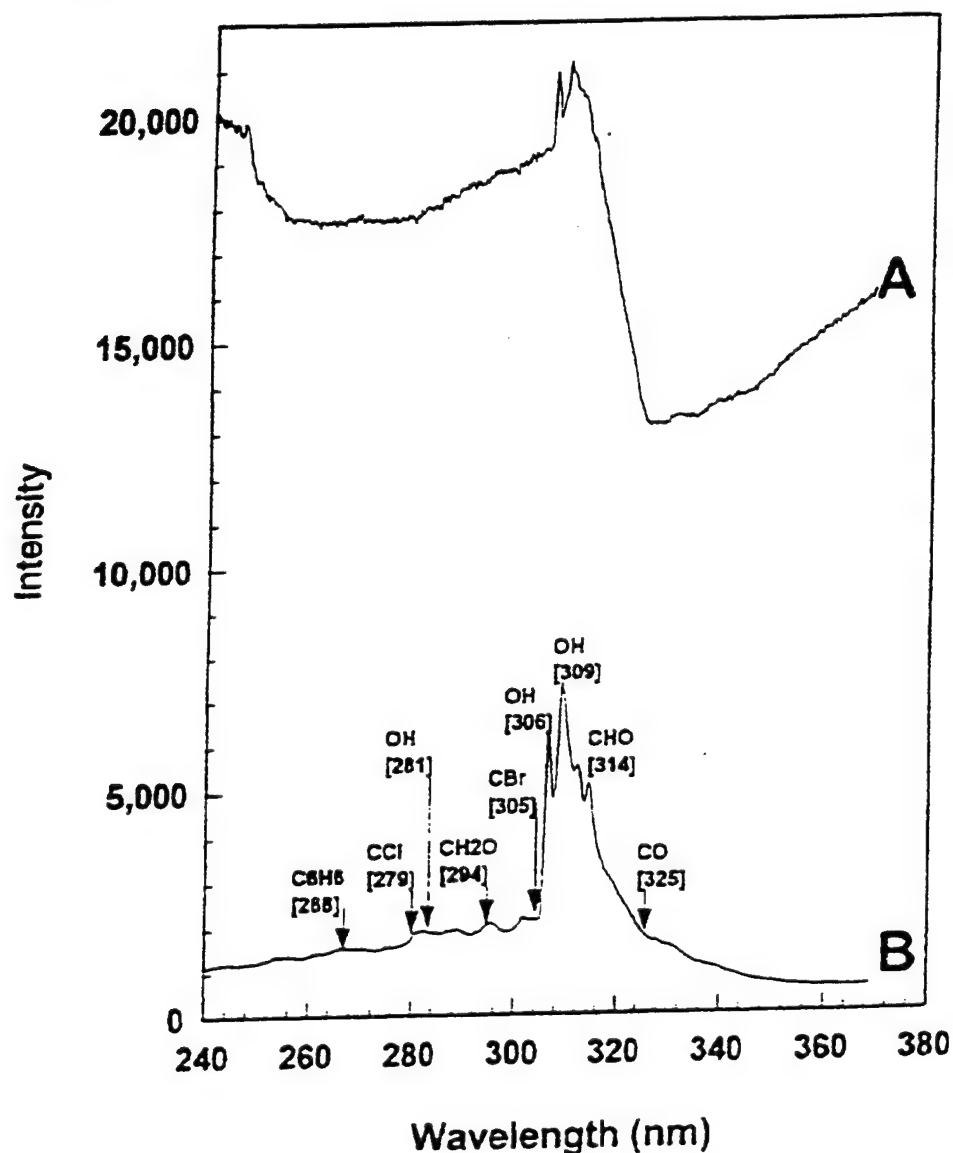


Figure 14. (A) MUV spectra of a propane diffusion flame with halon 1211 added to the fuel stream. (B) similar case with good stray-light-rejection measures with tentative identification of molecular features.



#### D. SUPPRESSION OF PAN FIRES

Using the improved stray light system we have obtained reasonable UVV and UV spectra of laboratory sized pan fires of three types of liquid fuels: (a) oxygenated fuels such as methanol and ethanol; (b) pure hydrocarbons such as hexane and heptane and (c) blended hydrocarbon fuels such as JP4, diesel, gasoline, kerosene and others.

The major effect of increasing the concentration of 1211 suppressant in a methanol pool fire observed in this initial effort was the gradual increase in the visible Planck continuum. The increasing soot formation as halon is added changed the flame from a typical blue flame to an increasingly yellow to red flame. In the MUV a decrease in the intensity of the OH band was observed as the halon concentration was increased. This initial survey of UVV and UV spectra of burner and pool fires without and with halon 1211 and 1301 suppressants revealed several potentially useful properties of flame - halon suppressant interactions:

(1) Molecular species including free radical are very apparent in the emission of premixed burner fires or methanol pool fires in the UVV and in the MUV.

(2) Diffusion burner flames or pool fires of pure hydrocarbons (e.g., heptane) or fuel blends (e.g. JP-4) have a strong black body (Planck) continuum in the visible and near infrared. The injection of halons into diffusion burner flames and pool fires enhances the black body continuum.

(3) The MUV spectra of the flames in (2) still show free radical molecular features when precautions are taken to reduce the stray visible light that makes its way to the MUV CCD channels.

(4) Metals, such as sodium, potassium and other strong emitters, if present in the fuel, can readily be observed as sharp lines in the emissions of the flame itself. Copper seeding appears to make halogenated molecules more readily observable.

This study builds upon the above exploratory study [9] and the MS Thesis study of Dale Walter [11] by: (a) using aerosol as well as halon suppressants (b) concentrating on the MUV region (c) using an improved spectrometer and blocking filter to achieve better stray light rejection, (d) using an improved pool fire and suppressant injection arrangements (e) using energy analysis and kinetic modeling to seek a semi-empirical interpretation of experimental observations.

In our prior work on monitoring the ozone optical depth and solar UV-B [25] stray visible light often overwhelms the true ultraviolet sunlight radiation. Fortunately, the same stray light rejection techniques that we pursued in solar ultraviolet radiation are useful in investigating the MUV spectra of flames. Indeed the visible light blocking filter used here was designed for use in a solar UV program. In this work we use additional internal baffling to avoid overfilling spectroscopic element, black velvet to absorb zero order reflections and other internal spectrograph improvements.

These experiments also strived to achieve more careful control of experimental conditions including the use of an improved pool fire, an improved suppressant delivery system, an improved positioning system for fixing the portion of the fire focused into the slit and other improvement that hold significant variables to tighter limits.



Figure 1 of Section I shows the apparatus used in our initial pool fire spectroscopy set up. We impose a separation between the liquid fuel and the flame by establishing an air free zone above the liquid which is heated to boiling by a hot plate. The suppressant enters the fire just above the surface of the liquid fuel and mixes with the fuel vapor prior to combustion. Gaseous suppressants are metered with a calibrated rotameter. Aerosol suppressants are applied by a piston moved at a precisely defined rate in a firing chamber previously filled with pyrotechnically generated smoke. The experiments are conducted in a hood to draw away the toxic products of flame-suppressant interactions. A half cylindrical shield around the fire stabilizes the flames from excessive turbulence caused by the hood fan.

Figure 2 of Section I (curve a) gives the UV spectra of a heptane pan fire taken with a standard blocking filter with minimal visible and near IR transmission but good MUV transmission. These spectra were taken before extra stray light rejection measures in our spectrograph were implemented. The major peaks near 306 and 309nm belong to the OH (0-0)  $\Sigma - \Pi$  transition. Other molecular features are apparent above 310 nm and below 300 nm. Figure 2 (curve b) shows the same spectral region when a pyrotechnically generated aerosol suppressant is added. The change parallels somewhat changes seen in our study of flame-halon suppressant interactions. The atomic feature near 406 nm is due to potassium.

Not seen in Figure 2 is the large visible continuum a common feature of diffusion flames particularly when suppressants are added. Some features in Fig. 2 reflect stray light (the spectra was taken before spectrographic improvements were made). To improve the identification of molecular features when signal to noise ratios are close to unity we used some of the digital manipulation available with our spectrometer - computer system.

#### E. METHANE - 1301 SPECTRA

In view of calibration problems with our initial propane - suppressant studies using the 400 line/mm grating we have carried out similar investigations with separate gratings and with careful attention to calibration [27]. Figure 15 A shows the spectra taken with the 400 l/mm grating of the region of a premixed natural gas flame (mostly methane) at the top of the cones. A gas flow rate of 1.2 liters/min and an air flow rate of 10 liters/min provides our reference flame. Figure 15B shows the spectra of the same region with the injection of 72 ml/min of halon 1301. The enhancement of the visible and near infrared regions with halon injection and the decline of the OH feature near 306 nm are noteworthy. Figure 16 shows the MUV spectra of the same flames obtained using a 2400 l/mm grating. Figure 16A is without halon and Figure 16B is with halon injection showing more clearly the reduction of the OH features with halon injection.

As already noted in diffusion flames (no premixed air) the Planck continuum is much larger than in premixed flames. Under fuel rich conditions, soot formation occurs and the flame is bright yellow as opposed to the blue color of the soot-free premixed flame. As described in our earlier study [10] we use a solar blind filter (SBF) with a 230 to 340 nm band pass (Corion SB 300-F) that further rejects VIR emissions. Figure 17A illustrates the MUV spectrum of a diffusion flame without the SBF. Here the count in each channel is divided by 4 to maintain the same scale as in 3B (with SBF) and 3C (with SBF and halon).

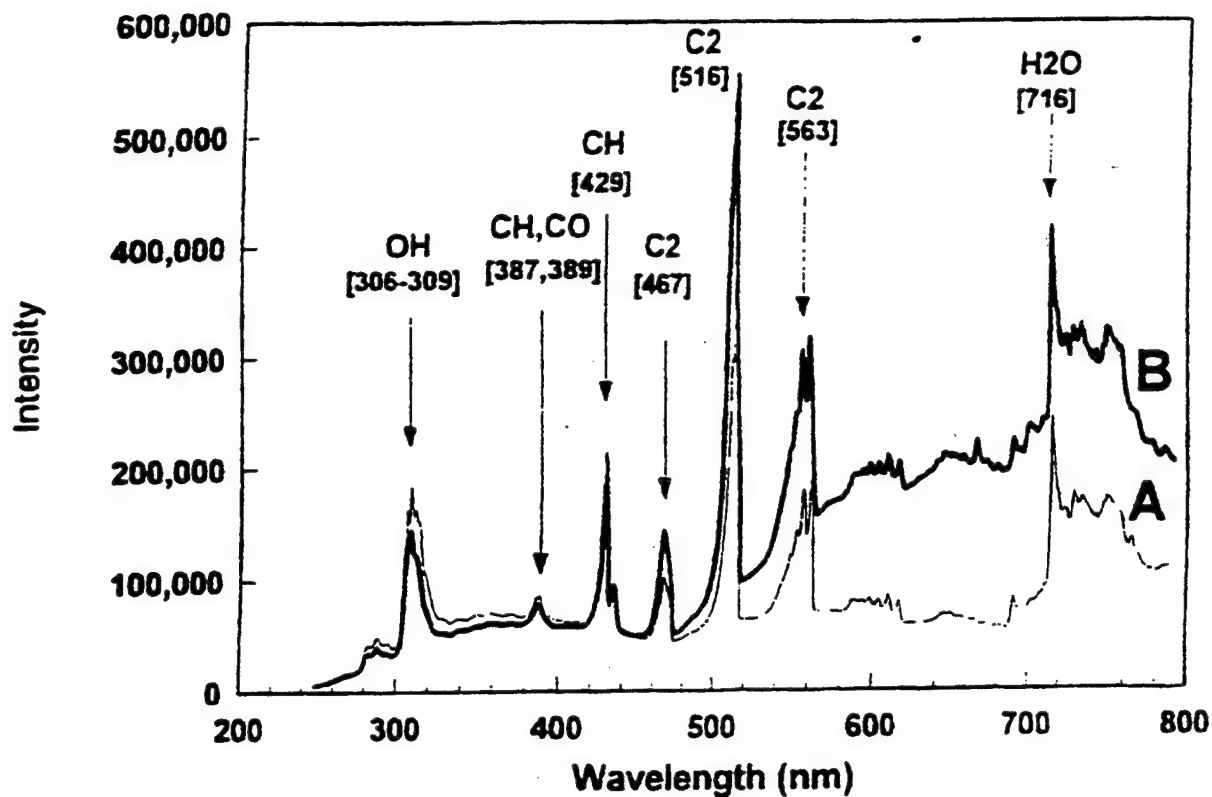


Figure 15. Premixed methane-air flame spectrum taken with 400 l/mm grating (A) without halon, (B) with halon.

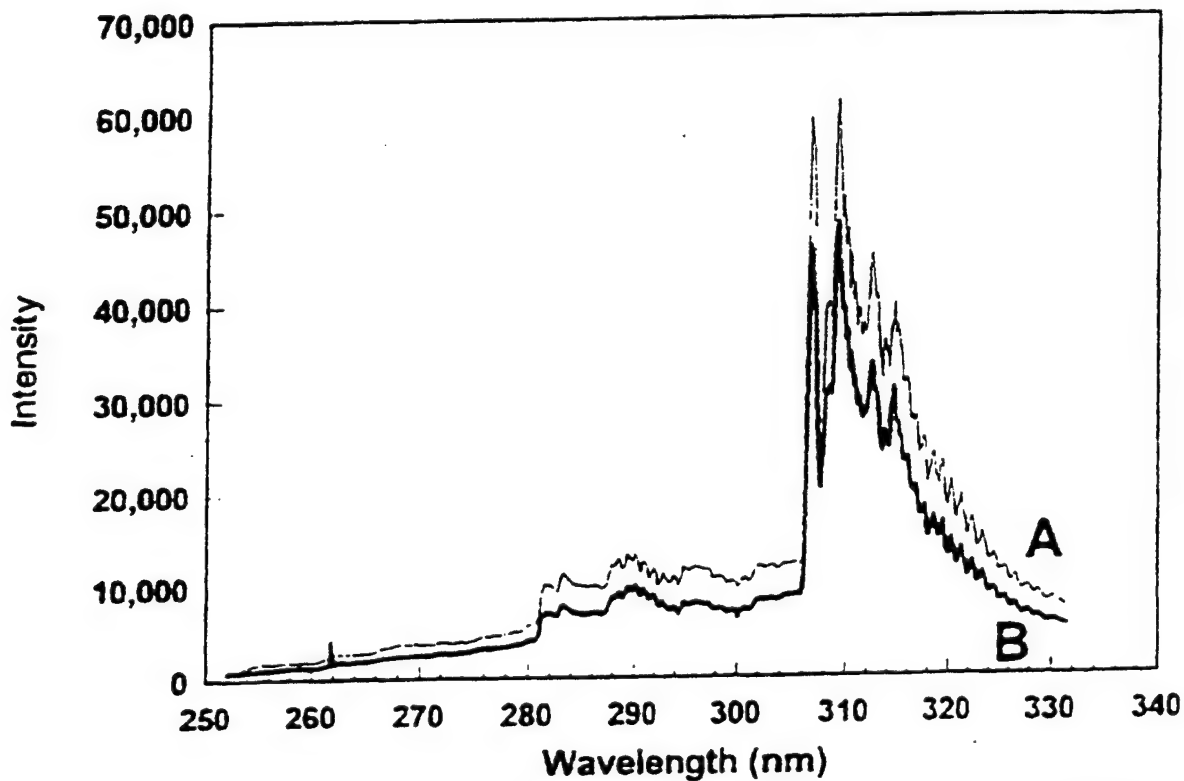


Figure 16. Premixed methane-air flame spectrum taken with 2400 l/mm grating (A) without halon, (B) with halon.

The decline in the 306 nm OH band with 1301 injection is observed in Figure 17 as in Figure 16 and less clearly in Figure 15. The decrease in OH emissions with increasing suppressants despite the increase in the VIR components of the spectrum is again suggestive of free radical scavenging.

The spectra illustrated in Figure 15, 16, and 17 do not make use of the two dimensional capabilities of current multichannel spectroscopy with CCD detectors. This can be accomplished with our imaging arrangement by dividing the 256 vertical rows of pixels into 5 to 10 groups or by using 5 to 10 fiber optic cables to convey various vertical section images of the flame to the spectrograph entrance slit. For quantitative work the image plane should be flatter than is the case with our spectrograph but spectrographs are now available with such a feature.

As noted earlier during the course of the CCTL fire suppression studies several halon extinguishment mechanisms not considered in the TH and FR approaches were encountered [11]. These include (a) the increased blackbody radiation, (b) the increased soot formation, and (c) the increased CO production. The decreased combustion efficiency, due to increased carbon monoxide and soot production as well as the increased radiation are cooling mechanisms that contribute to flame extinction. Pool fires of common oils can radiate 40% or more of the total heat release rate. For small pool fires this fraction increases to as much as 50% of the fuel energy release rate when halons are added [11].

In this methane - halon study the total output radiation of our premixed and diffusion flames are measured with a thermopile radiometer at several different rates of halon. We used a thermopile placed 150 mm away from the fire that viewed the methane flame broadside at the same height as viewed end-on by the spectrometer. The large acceptance angle of the radiometer makes the total radiation measurements less susceptible to changes in flame structure than spectral measurements. Figure 18 shows the thermopile voltage output for the premixed and diffusion flames at various halon injection levels.

## G. KINETIC MODELING OF METHANE FLAME SPECTRA

An important limitation on our ability to interpret the middle ultraviolet spectra of flame-suppressant interaction is the lack of reaction rates leading to the  $\Sigma$  excited state of the OH radical. In an effort to stimulate quantum theorists to undertake calculations of such reactions. Green and Xue carried out some exploratory kinetic modeling of the emissions of methane -1301 flames using "for instance type" reaction rates.

Main frame computers, minicomputers and even PC's can now solve large numbers of simultaneous differential equations that arise in kinetic models of combustion. Note that to follow H and  $H_2$  concentrations when hydrogen passes through a temperature-time cycle would require following  $2 \times 2 = 4$  reactions. For hydrogen and oxygen reactions, if we consider the stable species  $H_2$ ,  $O_2$  and  $H_2O$  and the intermediate free radicals H, O, OH, and  $HO_2$ , we must follow  $7 \times 7 = 49$  reactions. If one goes to hydrogen, oxygen and carbon chemistry, the number of species and reactions that could play a significant role increases greatly.

In this study, we simply follow the fate of 10 additional species,  $CH_4$ , C, CH,  $CH_2$ ,  $CH_3$ , CO,  $CO_2$ , CHO and  $CH_2O$ , we must, in principle, contend with a total of  $17 \times 17 = 289$  reactions. If we add  $C_2$ ,  $C_3$ ,  $C_4$ , etc. hydrocarbon compounds to the reacting pool the number of species to be followed increases rapidly and the number of reactions

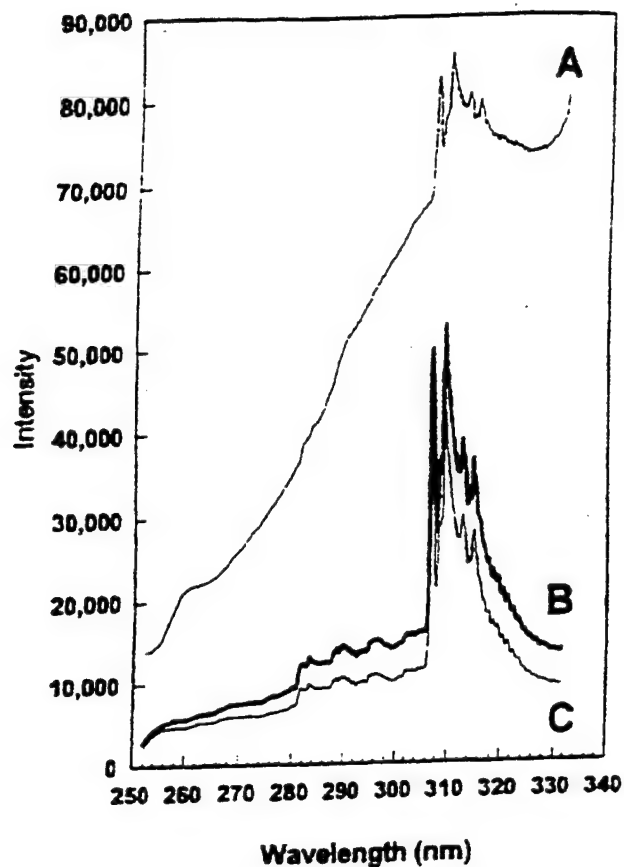


Figure 17. Diffusion flame spectrum (A) without solar blind filter (counts divided by 4) (B) with solar blind filter (C) with solar blind filter and halon

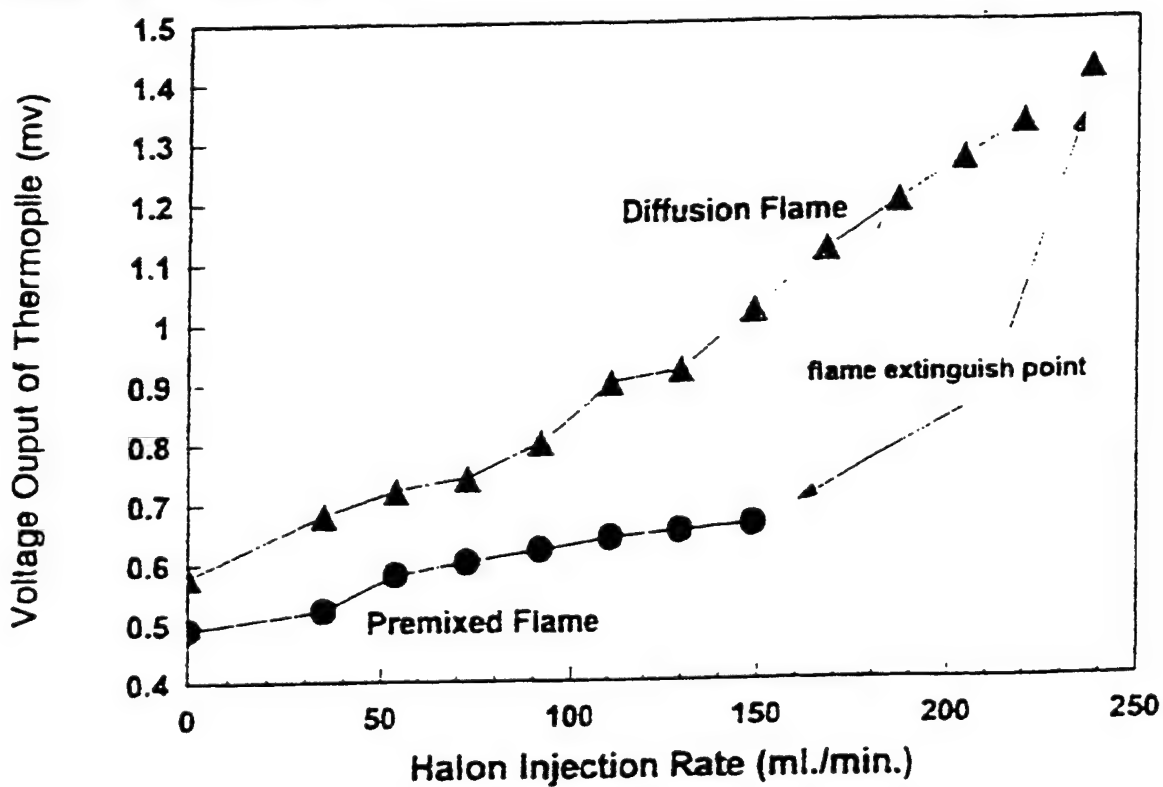
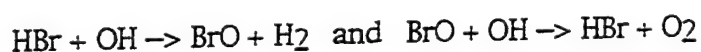


Figure 18. Voltage output of thermopile vs. halon injection rate

proliferates tremendously. Suppose now one wishes also to follow the evolution of simple halogenated species (X); where X can represent the halogens F, Cl, Br, or I; that might arise from the injection of halons. These could include, for example, X, X<sub>2</sub>, HX, OX, CX, as well as polyatomic combinations of X, H, O and C. The number of reacting species might then reach to 100 and the reactions to 10,000. It will take many years before these reaction rates are measured and clearly the solution of such sets of kinetic equations could only be carried out with large computers.

The traditional approach in the application of kinetics to flame studies has been to await the measurement of individual reaction rates before undertaking calculational experiments that include the species involved. Unfortunately, this tradition postpones to the distant future the day that kinetics can contribute to our general understanding of some real world problems. These include the cocombustion of fuels [28] the generation of organic toxics [29-31], the scavenging of ozone depleting species and greenhouse warming species by atmospheric OH radicals or as in this study fire suppression mechanisms. An alternative approach is to take a very selective path in a multidimensional {H, O, C and Xs} species space based upon experimental evidence and best guesstimates as to the key involved species. Such ventures into H, O, C, Cl space in studies of toxics generation [29-31] have led to simple phenomenological kinetics models roughly compatible with experiment.

In our kinetic studies of suppressant effects we have taken a standard collection of reaction rates for simple H, O and C combinations and considered very selective sets of additional reactions when Br is added to the input. For illustrative purposes we have focused our attention on simple models leading to the formation of HBr that catalytically destroys OH radicals via the hypothetical cycle



Our hope has been to gain some insight into the pattern of reaction rates needed to achieve order-of-magnitude agreement with our experimentally observed emission spectra. Essentially we seek simple models that can describe the response of methane burner flames when acted upon by halon 1301. We assume HBr enters via the reaction  $\text{CF}_3\text{Br} + \text{H}_2 \rightarrow \text{HBr} + \text{CF}_3\text{H}$ . We particularly consider the gas phase production of OH radical formation in the ground and resonance excited state (OH\*) and how it might be impacted by HBr. We impose a temperature-time profile roughly compatible with our previous experimental experience with flames [28-32]. These can be represented by the analytic expression

$$T = T_0 \exp t/t_1 \exp -t/t_2 / (g + \exp t/t_1)$$

where  $t_1$ ,  $t_2$ ,  $g$  and  $T_0$  are empirical parameters chosen to fit experimental data or general experience. In this methane burner case such a temperature-time profile is followed for 20 ms which will generally take a gas parcel through the top of the flame. Nineteen basic species were followed and sixty reaction between these species were included in the code for the basic H-C-O combustion reactions as compiled from various sources [28]. We include a hypothetical reaction  $\text{H} + \text{HO}_2 \rightarrow \text{OH}^* + \text{OH}$  where OH\* is the hydroxyl radical in its 4 eV electronic state (<sup>2</sup>Σ). With this simple scheme and judicious choices of unknown reaction rates our kinetics model gives results that simulate our MUV spectra. Figure 19A and 19B show the species evolution of gases in a premixed CH<sub>4</sub> flame representative of our experimental set up. Figure 19C and 19D give the corresponding species evolution patterns when a small concentration of CF<sub>3</sub>Br is added to the input to provide HBr and cyclic OH destruction reactions.

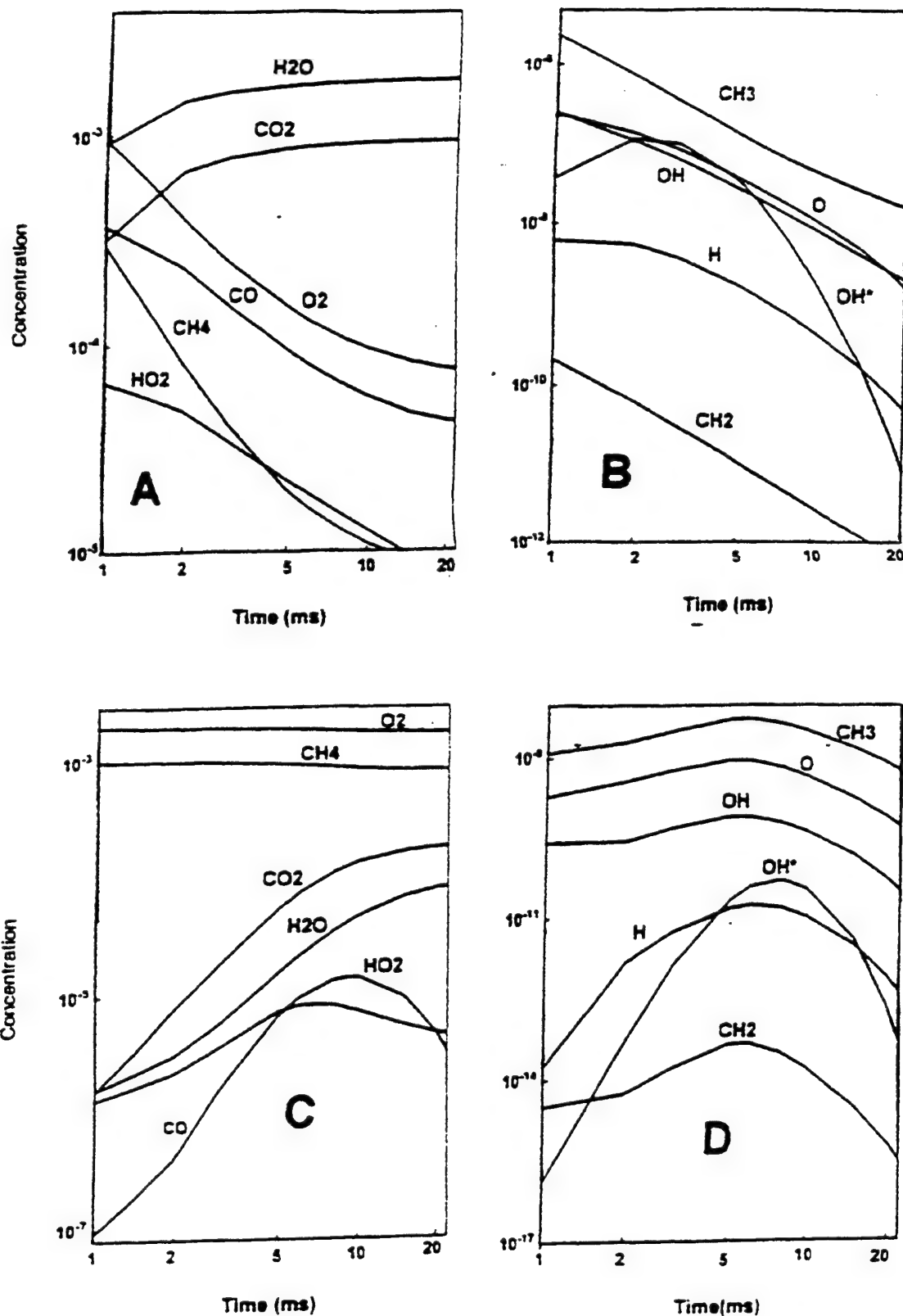


Figure 19. Kinetic model results for premixed methane flame with assumed temperature-time profile (A) major species, (B) free radicals and minor species, (C) major species when halon 1301 is injected, (D), free radicals and minor species when halon 1301 is injected (note changes in vertical scales).



In generating Fig. 19 we have used an empirical temperature - time function based upon thermocouple measurements at various heights in the flame and estimates of the height vs time of parcels of gas in the burner. However coupled fluid dynamics-chemistry codes are now available [33] that, given input flows, can approximately calculate the temperature vs height and time of simple burner flames. Alternatively we could use the stroboscopic illuminated magnesium oxide technique of Lewis and von Elbe [34] to establish an experimental height vs time function. Then measured temperature vs height profiles lead to temperature vs time functions that facilitate kinetic modeling. If reaction rates to the excited states of free radicals were available it should be possible to correlate observations of MUV spectra vs height with and without suppressants with that inferred from kinetics calculations.

A major obstacle to the calculation of the middle ultraviolet spectral emissions of the simple molecules of interest in fire and fire suppression research is the lack of knowledge of collision cross sections leading to the observable free radical species in excited electronic states lying from 3 to 6 eV above their ground states. These collision cross sections, if known, can be directly transformed to reaction rates [22,35]. Of particular importance are cross sections or reaction rates leading to the  $2p$  ground state and  $2\Sigma$  excited state of the OH radical.

The oxidation of hydrocarbons takes place largely through a succession of reactions involving attack by free radicals on unfragmented molecules or on their intermediate decomposition products. At combustion temperatures reactions involving OH radicals are the most important chain-propagating steps with reactions of O atoms and H atoms of secondary and tertiary importance. Cohen [36] has applied conventional transition state theory to the reactions of OH, O and H with alkanes and develops good frameworks for the extrapolation of their rate coefficients to regimes beyond the range of measurements. An intensive survey of the literature of cross sections or reactions rates leading to OH products [37-39] indicates that while many reaction rates (often inconsistent) are now listed practically none leading to electronic excited states are available. Nevertheless calculations of such cross sections appear within the current range of quantum chemistry.

Truhlar and Garrett [40] have recently reformulated transition state theory using quantum mechanical resonance theory. Such models have long been used in nuclear theory where collisions leading to compound and product nuclei in excited nucleonic states are readily observable by particle and photon (gamma ray) energy and intensity measurements [41]. It appears likely that techniques used in nuclear scattering theory (see also references 26 in [40]) could serve for the calculation of the OH radical  $2\Sigma$  state emissions from flames. These emissions are uniquely observable signals of important free radical action in flames even when large black body emissions are present. If resonance scattering theory formulations are adaptable to the relatively few important reactions leading to OH production in its  $2\Sigma$  excited state a focused program of quantum chemistry calculations should be helpful to the interpretation of MUV OH emissions from flames with and without suppressants.

In our view such a calculational program should first consider halon suppression in hydrogen flames. In this case the reaction rates to be studied might best be ordered by three and four body complexes, as illustrated in Table 6. Considerable data is available to test theoretical calculations of reaction rates to ground states (see, for example, very recent reaction rate listings by Leung and Lindstedt [42]). The computational effort would be useful not only for flame studies

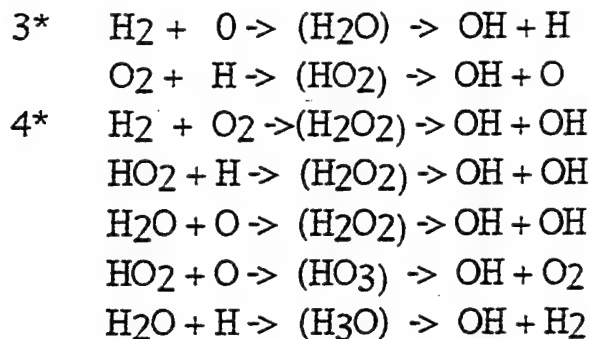


but also for interpretation of the chemistry subsequent to charge particle deposition in water [43].

For methane flames since a number of dissociation products play roles in high temperature oxidation many more reactions lead to hydroxyl radicals as products than in the case of hydrogen flames. Again it is suggested that reaction rate calculations first be prioritized by the collision complex as shown in Table 7. Reductions in the number of rate constants that are needed can be established by consideration of energetics and by examination of principal pathways [44].

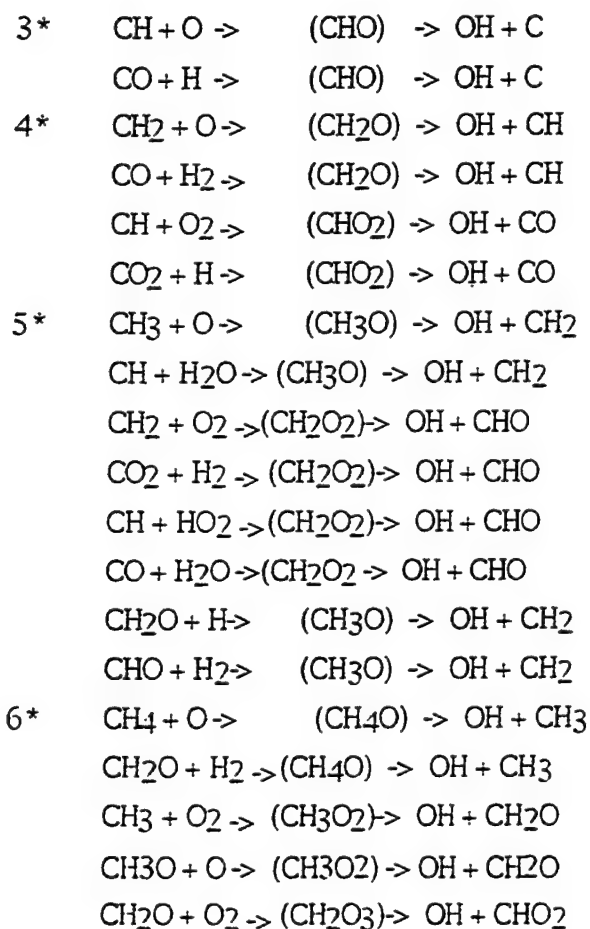
While calculating rates for the reactions listed in Tables 6 and 7 might represent a formidable task, a focus on the OH radicals might have other useful by-products to justify the effort. These radicals are the scavengers of methane and many other anthropogenic gaseous emissions involved in global warming and ozone depletion [45]. Thus the more known about the generation of OH radicals the more this knowledge might also be applied in strategies to mitigate climate change and ozone depletion, two global environmental problems of major international concern.

Table 6. Reactions in hydrogen flames leading to hydroxyl radicals



\* number of atoms in collision complex

Table7: Reactions in methane flame leading to hydroxyl radicals



\* number of atoms in collision complex

## SECTION VII

### DISCUSSION AND CONCLUSIONS

#### A. FLAME SUPPRESSION

##### 1. The Understanding of Flame Suppression

As indicated in Section I, II and VI the lack of understanding of fire suppression mechanisms has been a serious impediment to the search for halon alternatives [1]. The halon free radical (FR) scavenging mechanism has been questioned by Ewing et.al, [2,46] and recently challenged again by Larsen [1]. Thermal mechanisms (TH) do not generally achieve the high extinguishing effectiveness that one expects from catalytic type chemical mechanisms. Thus if the primary flame suppression mechanism of pyrotechnically generated aerosols is strictly thermal there will be limits to weight and size reductions in the design and construction of hand thrown devices. An improved understanding of the physical and chemical phenomena involved in fire suppression clearly would greatly help guide the selection among potential alternatives. It would also help choose the directions for future improvements and optimization efforts. .

If the fire suppression mechanism is primarily free radical scavenging then cyclic catalytic reactions that convert free radicals to more stable forms could multiply the effectiveness of the pyrotechnically generated aerosols. This should reduce the quantity of suppressant needed to put out a given sized fire. If PGAs work thermally additives to the SFE propellant that would cause free radical scavenging could be helpful.

##### 2. Radiation - FR - Coupling

By many measurements of MUV OH emissions with our computer spectrograph we have direct evidence showing the decrease of OH with halons and SFE aerosols. By direct measurement we have shown that total radiation increases with halon and SFE injection. These observations have led us to explore the possibility of a coupling mechanism between radiation and free radical scavenging (FRS). With the help of the literatures on the emissions of toxics and soot from the combustion of chlorinated organics we believe we have found a physical and chemical basis for such a coupling.

A halogen atom X can react with a hydrocarbon molecule RH leading to



This extraction of H from the hydrocarbon by the halogen fosters nucleation of the more carbonaceous residue R [24]. Nucleation initially leads to very fine particles which enhance the radiative efficiency of a given mass of particles. This follows from the simple argument that the total area per unit volume of a concentration (n) of spherical particles is [in particles per unit volume]

$$A = 4 \pi r^2 n$$

where r is the particle radius. On the other hand the mass per unit volume is

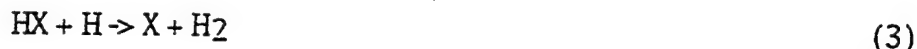
$$M = (4\pi/3) r^3 n \rho$$

where  $\rho$  is the density of the particle. Thus the radiation per unit volume is

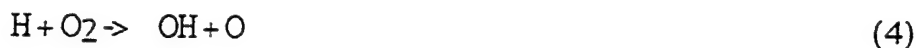
$$R = \epsilon \sigma T^4 A = \epsilon \sigma T^4 3M/r\rho \quad (2)$$

where  $\epsilon$  is the emissivity and  $\sigma$  is the Stefan Boltzman constant. Since nucleation leads first to very small particles the radiation loss near onset could be very large.

The halogen acid HX formed by reaction (1) can scavenge hydrogen radicals via [3]



thereby recycling X to a pool that fosters nucleation. Thus nucleation or soot formation is associated with the rapid exhaustion of H radicals. In hydrocarbon combustion the exhaustion of H radicals interrupts the important branching step [2]



thus lowering the concentrations of OH and O.

The coupling of sooting-enhanced radiation and free radical scavenging (to be referred to as the RFRSC hypothesis) can add significantly to the dilution, heat capacity decomposition and vaporization invoked in thermal (TH) loss hypothesis of Ewing et al [2]. Accordingly we believe our spectroscopic and radiation measurements points to a possible resolution of the TH vs FR controversy with a mechanism that is intermediate between both theories.

It might be noted that our key word searches of the literature since 1990 failed to reveal prior work connecting radiation enhancement with reduced free radicals. We found the missing links in our RFRSC hypothesis in the literature on toxics and sooting associated with the combustion of halogenated hydrocarbons.

### 3. Hydrogen - 1301 Flames

To address questions raised by our RFRSC hypothesis and set the stage for more intensive theoretical interpretations of flame-suppressant interactions, Xue and Green [48] initiated measurements of the spectra and total radiation of hydrogen diffusion flames at various concentrations of halon 1301. Studying hydrogen flames rather than hydrocarbon flames substantially reduces the species involved in combustion reactions. It also simplifies the intended theoretical kinetics modeling by reducing the number of reactions that lead to OH radicals in the ground and resonance electronic states (See Table 6 and 7).

Unfortunately we ran out of halon 1301 and also out of time before completing our hydrogen flame study. However we obtained rather provocative preliminary results at four levels of halon injection rates. Visually we observed our hydrogen diffusion flame to be dim and light red. When halon is injected at a

low rates it turns a bit blue and at a higher rate it becomes bright yellow. Just before extinguishment, it is very bright like a candle.

We have calculated the flame radiation rate after the thermopile was calibrated with a quartz halogen lamp. We concluded that ratio of hydrogen diffusion flame radiation to total released energy goes up from 18%, in the case of no halon injection to over 33%, when the halon 1301 level is close to the extinguishment point.

The hydrogen flame spectroscopy and radiation experiments thus also suggests the RFRSC hypothesis. Since in this case the fuel cannot contribute carbon the possibility that the halon itself releases its carbon bears investigation. Alternatively non-carbonaceous nucleation might be involved.

#### 4. Benign Sources of Fine Aerosols

Two years ago the principal investigator conducted an unfunded study of fire suppression by solid particles contained in phosphate slimes. Using these slimes we adapted pressure fire extinguishers to propel water mists loaded with colloidal phosphate particles. While conducting an unfunded study with students is not a promising way of investigating hardware possibilities we did observe some promising results. Thus when we extinguished 12" diameter oil fires we found results that were judged to be better than the use of water itself by a professional from our Safety Division (Gordon Wilson).

In the course of the phosphate slime effort the PI constructed a soft ball of semi-dried clay packaged in a thin plastic bag. The intent was to surround this package by a layer of gunpowder (Mark 1) to accomplish passive ignition. A second version (Mark 2) was to be investigated in which a central core of gunpowder insured dispersal of the fine clay particles. Unfortunately gunpowder was not acquired until the semester ended and the students had graduated. A third type of device was considered in which a pyrotechnical pressure generator is used to atomize the phosphate lime slurry but it was not implemented for lack of time.

With the initiation of the Task 3.06 - 3.08 project we focused our energies first on the EMAA canisters already fabricated by Spectrex. We also considered engineering options derivative of the products of Martin Electronics, Inc. in Perry, Florida. Since neither of these directions looked promising as a basis for a hand thrown 500 gram SFE device we launched a broad survey of all models members of the CCTL could come up with and build with reasonable expenditures of time and money. Many of these prototype firings were captured with our rather primitive video set up using a camera discarded by our Journalism College. The tapings were primarily intended for in house use, however, they obviously contain considerable extra information that was used in reaching the conclusions of this report. A log of these firings and a video tape are available by special request to the principal investigator.

In retrospect we should have continued our investigations with colloidal particles in phosphate slimes. The material is available at no charge, the water carrier would be an energy sink, rather than a high energy source as SFE and the particle sizes are in the submicron range greatly fostering the radiation loss mechanism.

## B. DESIGN AND CONSTRUCTION OF HAND THROWN SFE CANISTERS

In this project we were given a 500 gram (1.1 lb) SFE-type charge that pyrotechnically generates solid particulate suppressants and releases about 2400 BTU. We were to cool its output (equivalent to boiling 2.4 pounds of water) in a minute or less and retain the flame in a hand thrown device. Among the potential approaches examined for cooling, flame retention, and shock resistance in a throwable device several appear potentially viable if a Device / SFE weight ratio of 6 or greater is acceptable. These include:

1. (MWCD) SFE: aerosol cooling and flame baffling through a multichannel water embedded and sealed ceramic passageways leading to a cooled wet aerosol
2. (MFTB) SFE: aerosol cooling and flame baffling via a multichannel fire-tube boiler system leading to a cooled dry aerosol and a separate steam exhaust
3. (CHRD) SFE: cooling with dolomite blending to generate aerosols with CO<sub>2</sub> and while retaining heat in the CaMgO<sub>2</sub> residue and also with some MWC or MFT cooling. Such devices generate aerosols and gaseous suppressants.
4. (RCBD) SFE: flame radiation through mica like windows with baffles for the flame and some passageway cooling for the aerosols.

On January 12, 1995, we achieved a Device/SFE-charge (D/C) weight ratio of 6 using 500 grams of SFE. Since it would have been difficult to substantially lower this ratio by further experimentation within our capabilities we focused our attention on modeling studies. These were intended to examine methods of minimizing the D/C ratio with MWCD and MFTB type devices using the heat transfer analyses given in Sections III and IV.

We have concluded that it would be very difficult to fabricate hand thrown devices with (D/C) weight ratios substantially less than 6 with SFE charges. This conclusion would be altered if a suitable aerosol generator with lower heat release rate can be found. Alternatively if SFE can be blended with a heat absorber that retains heat and enhances the fire suppressing qualities of the aerosols it might be possible to achieve a lower D/C ratio. Thus far our work suggests that blending with dolomite is the most advantageous heat absorber additive that might have enhanced fire suppression action by virtue of the CO<sub>2</sub> release.

During the course of our work we found a number of feasible general paths for using pyrotechnically generated aerosols in fire extinguishers. We also found many possible sub-paths that we could take, each with special features some of which are at the cutting edge of modern technology. Operations analysis was developed in World War II for this type of problem and has since evolved into Systems Analysis, Industrial and Manufacturing Science, Decision Analysis, Optimization Theory and other decision making fields. Heat transfer analysis is also becoming a well developed field and optimization programs are available. Accordingly the application of such techniques could help in the final path selection towards practical devices.

### C. POTENTIAL OFFSHOOTS OF PROGRAM

While attempting to meet the very severe requirements of a Hand Thrown Device we have developed several concepts that might serve other potentially important functions.

#### 1. Stationary Passive Flooding Device

Figure 20 is a schematic illustration of a possible SFE aerosol-CO<sub>2</sub> generator with a fire tube boiler type cooling configuration that might serve for passive applications. It would be mounted on the ceiling of a chamber to be protected. The steam generated is released horizontally and the aerosol is released downward. Some heat is retained in the CaMgO<sub>2</sub> residue. The fusing system and possible nozzles for the exhaust tubes to facilitate expansion cooling are not shown. These can be adapted in consideration of the devices used as fuses in weapons and in the triggering mechanisms used in sprinkler systems, smoke detectors, CO detectors and other alarm systems.

#### 2. Hand Held Fire Extinguishers

During our single channel studies we found that we were able to extinguish 6 inch diameter pool fires with small SFE charges by careful aiming or manipulation of the fanned exhaust. We constructed an externally cooled device capable of handling up to 40 grams and tested it on a 30 inch diameter diesel pan fire and it worked quite well. To insure that the extinguisher did not exhaust its charge before the pan fire was completely cornered and extinguished we provided a double fuel cylinder. This could be fabricated to facilitate quick recharging of the empty fuel cell while the fireman is still using the other cell to corner the flame.

In the laboratory we have tested externally cooled versions of such a fire extinguisher as illustrated in Figure 21. We have also tested an internally cooled system that used a wet ceramic cloth liner on the inside of the anti-fire gun. Both systems appeared equally effective during the trials made on laboratory scaled fires.

#### 3. Fire Diagnostics

Our ability to see free radical processes and toxic compounds in the MUV in smoky fires as illustrated in Figure 2 and hundreds of other spectra taken during this program has potentially useful applications in practical fire fighting situations. A more compact version of our spectrograph CCD system can be made by using the latest portable computer and some specially designed optical components. Such a compact portable system would make possible a number of field application of MUV spectroscopy. For example it might help a fire chief obtain immediate information on whether a fire is generating serious toxics or how close his suppression measures are to extinguishing the fire.

#### 4. RFRSC Hypothesis

Perhaps the most important by product of this research is an hypothesis that could bridge the gap between the thermal and free radical theories of fire suppression and thereby help the search for halon alternatives.



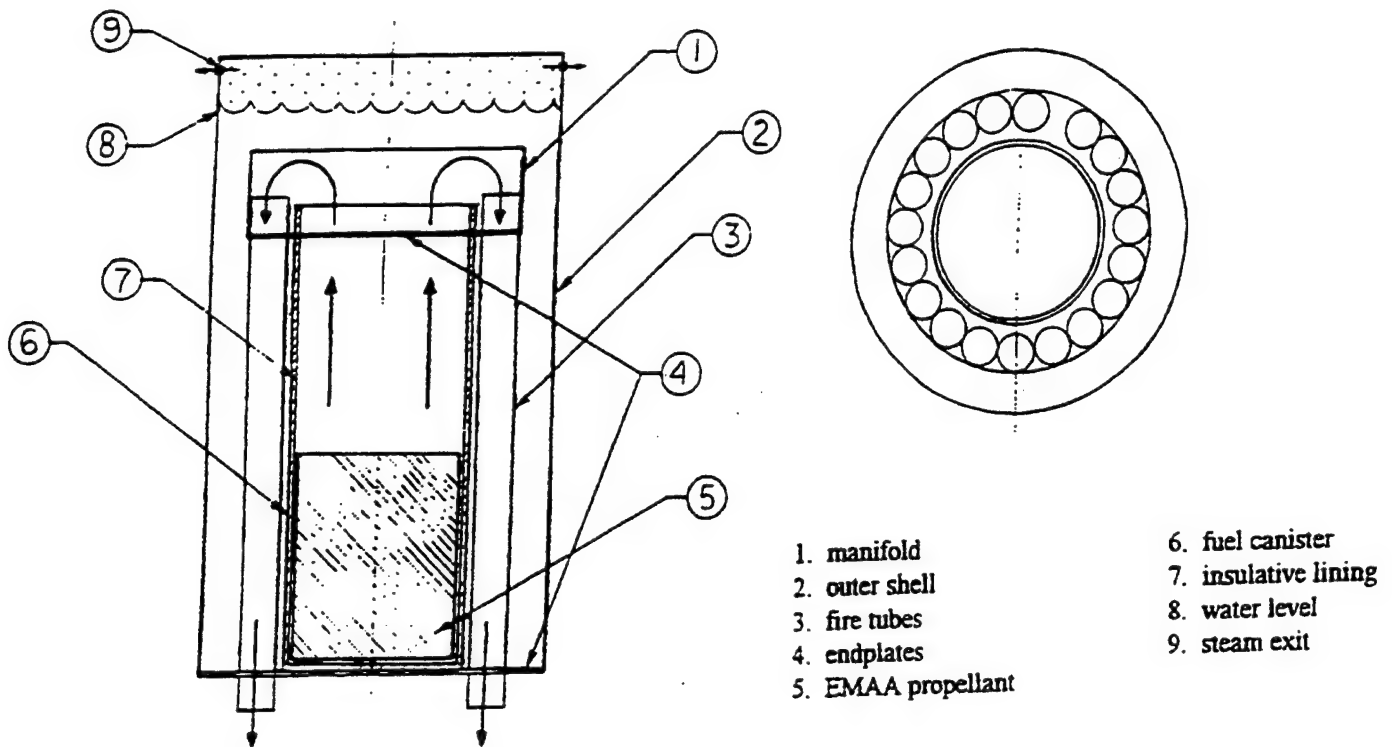


Figure 20. Multichannel fire - tube boiler (MFTB).

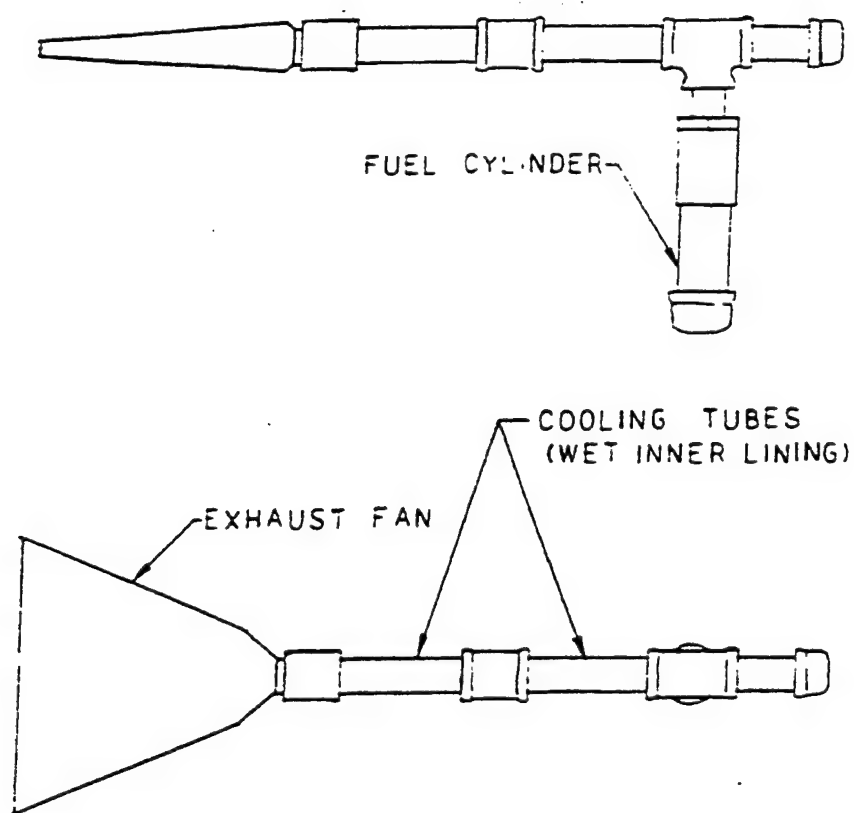


Figure 21. Hand fire extinguisher, exterior cooling.

## D. CONCLUSIONS

In relation to "Flame Suppression" (TASK 3.08 - sub task 2), we have observed correlations between increases in total radiation and decreases in OH emissions suggestive of a physical or chemical coupling between the two observables. We have developed a physiochemical explanation of this coupling and use the acronym RFRSC for "radiation- free radical scavenging- coupling to denote this hypothesis. One might try to invoke the thermal mechanisms of Ewing et. al.[2,46] to explain these coupled measurements but the fact that the radiation losses increase dramatically to higher than 30 % tends to contradict an explanation that temperature lowering can explain both observations. The specific links we invoked are supported by a vast body of data in the literatures on the kinetics of combustion, on soot formation and on toxic emissions from the combustion of chlorinated hydrocarbons. Accordingly our RFRSC hypothesis is supported by much more data than we have been able to assemble in this program.

Our RFRSC mechanism serves as a natural bridge between the strictly thermal hypothesis of Ewing et al [2,46] and the free radical scavenging hypothesis of Westbrook [3] . This should help resolve the differences between these two approaches leading eventually to a unified theory of flame suppression. Better understanding will provide a clearer set of properties to be sought in potential halon alternatives. However, much further work is needed to quantify the radiant emissions and other properties of flames when acted upon by potential suppressants near the extinction point of a particular fuel.

Subtasks 3 and 4 of Task 3.08, the design and construction of hand thrown devices charged with 500 grams of SFE, consumed most of our efforts through February 1995. By then we had examined and experimentally explored a large number of potential types of devices. We arrived at four major possible design paths (1) multichannel wet ceramic device(MWCD), (2) multichannel fire tube boiler (MFTB), (3) Carbonate Heat Retention device (CHRD) and (4) Radiation Cooled and Baffled Device (RCBD). We brought one path (multichannel wet ceramic devices) to a point that we thought was close to the best physical realization based upon a 500 gram SFE charge. This device had a (device/charge) weight ratio of about 6, contained the flame and produce steam-aerosol exhaust below the ignition point of class A and B materials (Video shot 41).

A second promising path that we brought close to practical realization is illustrated in Figure 22 (Video shots 15-18) that led to the lowest exhaust temperatures. In final form it would use a cylindrical aluminum radiator to finally absorb the exhaust heat. Our mock-up used 400 grams SFE and a segmented approximation to a cylindrical radiator. The devices we fabricated with segments of automotive radiators had large (device/charge) ratios. However with a professionally fabricated thin aluminum water filled radiator it might be possible to achieve approximately 6. If we combined this automotive type radiator use with features of our best MWCD approach we might be able to do a bit better.

The two cases illustrated in Figures 22 and 5 were the closest we came to devices with promising exhaust cooling and flame retention capabilities at the 500 gram SFE level. After February we devoted most of our efforts on Subtasks 3 and 4 to single channel tests and mathematical modeling with the objective of identifying more efficient heat absorption techniques leading to a cooler exhaust and a lighter device. This work essentially confirmed our earlier conclusions.

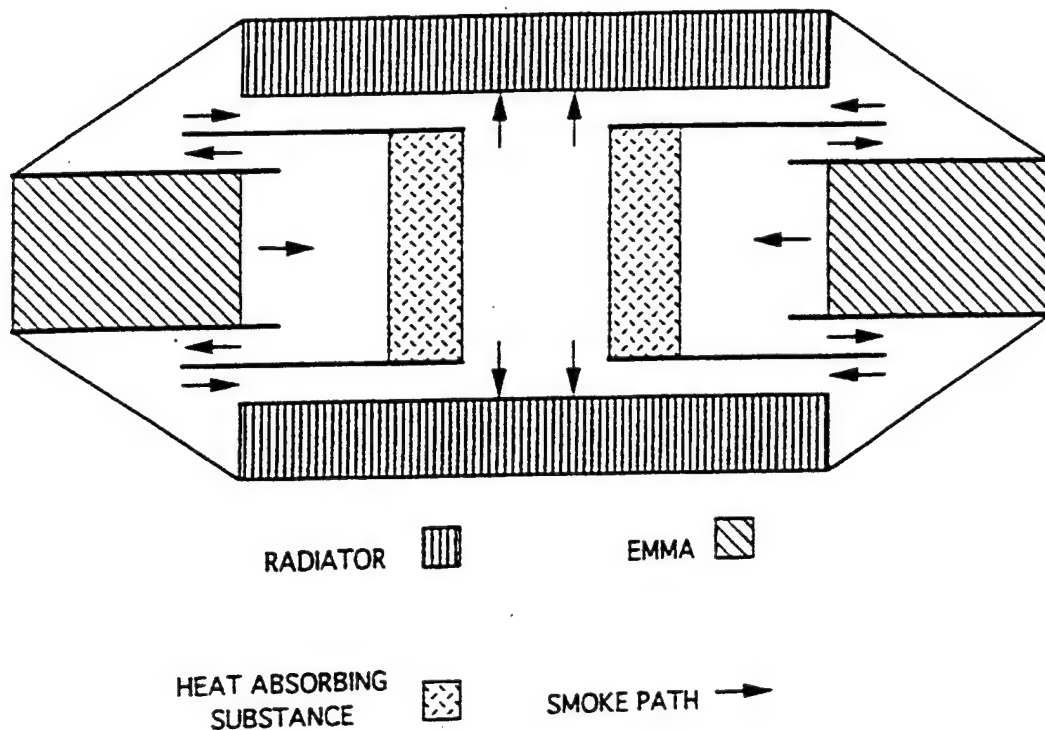


Figure 22. Illustration of a Possible Cylindrical Radiator Device

If one is confined to SFE charges it would be prudent in further R&D, to focus on stationary type devices or single channel fire extinguishers until successful experience with pyrotechnically generated aerosols in simple devices has been accumulated. Then this experience could be used to address the more difficult problem of designing and constructing hand thrown devices. Alternatively it might be prudent to seek more benign sources of aerosols or to use heat retention techniques combined with carbon dioxide generation.

Finally we must emphasize the importance of achieving a better understanding of the fundamental nature of fire suppression. Only with such an understanding could we apply operations analysis to arrive at a strategic decision among the many apparent options that could satisfy the objective of a hand thrown fire suppressant.

## E. ACKNOWLEDGMENTS

This document was prepared by the Clean Combustion Technology Laboratory of the College of Engineering for the Fire Testing and Research Center (FTRC) at the University of Florida under contract to Applied Research Associates (ARA), Inc., P.O. Box 40128, Tyndall Air Force Base, Florida, 32403, and the Air Base Fire Protection and Crash Rescue Systems Branch of Wright Laboratory (WL/FIVCF), Tyndall Air Force Base, Florida, 32403. The ARA Project Officer is Michael A. Rochefort, the WL/FIVCF Project Officer is Capt. Robert A. Tetla, the WL/FIVCF Section Chief is R. N. Vickers. For the University of Florida the project director is Dr. Weilin P. Chang director of the FTRC.

The Principal Investigator for this study was Dr. Alex E. S. Green, Graduate Research Professor of Mechanical Engineering and Nuclear Engineering Sciences in the College of Engineering and Director of the Clean Combustion Technology Laboratory (CCTL) and the Interdisciplinary Center for Aeronomy and other Atmospheric Sciences (ICAAS). Major contribution to Sections III and IV were made by James Mullin, partly in connection with his M.S. degree program in Mechanical Engineering. Important contributions to Section VI were made by Hui Xue, partly in connection with his M.S. degree program in Electrical Engineering. The work of Dale Walter, who completed his M.S. degree program in Mechanical Engineering in December 1994 is also reflected in this report. Other scientific and technical participants in this overall study include: Mr Donald Denniston, Drs. Theresa Miller and Juan Vitali, Cameron Harper, Charles Kibert Jr. and Douglas Tarbox. Gordon Wilson and Thomas Eadie formerly of the UF Safety Division contributed significantly by training us in oil fire fighting techniques and by providing halons for our experimental work. Manuscripts of monthly reports, journal and conference papers, the interim report of February 24, 1995 and this final report, were prepared by Freda K. Green. The work was conducted at the facilities of the Clean Combustion Technology Laboratory in the Space Sciences Research Building of the University of Florida.

We thank Bruce Green; who has served as an informal advisor-consultant and provided special ceramic materials critical to the work on the project. We also thank Emeritus Professor David T. Williams for his efforts on toxic detection using middle ultraviolet spectroscopy and Sergio Peres a member of CCTL laboratory who has helped this project on various occasions. The advice of other faculty members in Mechanical Engineering, Nuclear Engineering Sciences and Chemistry with expertise in related heat transfer problems and spectroscopy has also been most helpful. These include J. F. Klausner, C.K. Hsieh, D.Y. Goswami, G.J. Schoessow, S. Anghaie, J.D. Winefordner, B.W. Smith and R.T. Schneider.

Sincere thanks are also extended to Drs Winfred Phillips, M.J. Ohanian, William Tiederman, and James Tulenko of the College of Engineering, Vice Provost Gene Hemp and Vice President Karen Holbrook for flexible forms of research support some of which assisted this work. Finally we thank the Oriel corporation for the donation of several components of our experimental system,

## SECTION VIII

### REFERENCES

1. Freemantle, M., *Search For Halon Replacements Stymied By Complexities Of Fires*, ACS National Meeting in Anaheim, CA, Chemical & Engineering News, 1995.
2. Ewing, C.T., Faith, F.R., Romans, J.B., Hughes, J.T., and Carhart, H.W., *Flame Extinguishment Properties of Dry Chemicals: Extinction Weights for Small Diffusion Pan Fires and Additional Evidence for Flame Extinguishment by Thermal Mechanisms*, J. Fire Protection Engineering, vol 4, p. 35, 1992.
3. Westbrook, C.K. *Inhibition of hydrocarbon oxidation in laminar flames*, in Nineteenth Symposium on Combustion, Combustion Institute, Pittsburgh, PA, Comb. Sci. and Tech., 34, 201-225, 1983.
4. Green, A.E.S., Ed., The Middle Ultraviolet: Its Science and Technology, John Wiley & Sons, Inc., New York, 1966.
5. Berlad, A.L., *Radiation from Flames and Chemical Perturbations of the Atmosphere*, Chapter 12, Ibid 4.
6. Vaidya, D.B., Horvath, J.J. and Green, A.E.S., *Remote Temperature Measurements in Gas-coal Flames using the OH(0,0) Middle-UV Band*, Appl. Opt. 21, 3357 1982.
7. Pamidimukkala, K.M., Schippnick, P.F., Vaidya, D.B., and Green, A.E.S., *Ultraviolet OH Emissions in H<sub>2</sub>-Air Diffusion Flames*, JANAF 14th Plume Technology Meeting, Inkyokern, CA, Nov. 1983.
8. Horvath, J.J., Pamidi, K.M., Person, W.B. and Green, A.E.S., *Spectroscopic Observations of Methane-Pulverized Coal Flames*, J. Quant. Spect. Rad. Tran 31 1984.
9. Green, A.E.S., Walter, D.E., Vitali, J.A., Xue, H., Denniston, D., and Kibert, C.J., *Middle ultraviolet spectra of flames with aerosol suppressants*, presented at the Eastern Combustion Institute meeting and published in the proceedings, 1995
10. Green, A.E.S., Vitali, J.A., Walter, D.E., Kibert, C.J., *Middle Ultraviolet Spectroscopy of Suppressant-Flame Interactions*, Applied Optics, 34, 1607, 1995.
11. Walter, D.E., *Radiation of Small Pool Fires Suppressed by Halon 1211*, MS Thesis, University of Florida Department of Mechanical Engineering, 1994.
12. Miller T.L., and Green, A.E.S., *A Survey of Techniques for Fire Suppressant Studies*, in Proceedings: Halon Options Technical Working Conference, NMERI, Albuquerque, NM, May 3-5, 1994.
13. Sidorov, A.I., et al.; Russian Patent 192 669, 1967.
14. Spector, Y., *New Products Using Particulate Aerosols Technology (SFE)*, Ibid 12.

15. Kibert, C.J., Ranker, M.E., Sr., and Dierdorf, D.S., *Encapsulated Micron Aerosol Agents (EMAA)*, Proceedings: Halon Alternatives Technical Working Conference NMERI, pp. 421-432, Albuquerque, New Mexico, May 11-13, 1993.
16. Ball, D.N. and Russell, M.S., *Pyrotechnic Aerosol Extinguishing For AFV Engine Bays*, Proceedings: Halon Options Technical Working Conference 1994, NMERI, 1993
17. Sheinson, S., Eaton, H., Zalosh, R., Black, B., Brown, R., Burchell, H., Salmon, G., Smith, W., *Intermediate Scale fire extinguishment by pyrogenic solid aerosol*, Ibid 12
18. Jacobson, E., and Baratov, A., *Cooling Particulate Aerosols By Dry Extinguishing Powders*, Ibid 12.
19. Incropera, F.P. and Dewitt, D.P., Fundamentals of Heat and Mass Transfer, Third Edition, John Wiley & Sons, Inc., New York, 1990.
20. Lide, D.R., CRC Handbook of Chemistry, CRC Press, Inc., BocaRaton, 1991.
21. IANAF Thermochemical Tables, Second Edition, U.S. Department of Commerce, National Bureau of Standards, Washington, D.C., 1990.
22. Green, A.E.S., and Wyatt, P.J., Atomic and Space Physics, Addison-Wesley Publishing Company, Inc., Reading, MA, 1965.
23. Green, A.E.S., *The Middle Ultraviolet, Chapter 15 in Defense Conversion* A.Green and V. Cherny, editors, A. Deepak Publishing Co., Hampton, VA, 1995.
24. Glassman, I., *Soot Formation in Combustion Processes*, Twenty Second Symposium on Combustion, The Combustion Institute, Pittsburgh, PA, 1988.
25. Green, A., *Multi-Wavelength Determination of Total Ozone and Ultraviolet Irradiance*, Proceedings of the NATO Conference on the Role of Solar Ultraviolet, Copenhagen, Denmark, July 28-Plenum Press, NY, 1981.
26. Saunders, R.D., Kostkowski, H.J., Green, A.E.S., Ward, J.F., and Popenoe, C.H., *High Precision Atmospheric Ozone Measurements Using Wavelengths Between 290 and 305 nm*, J. Geophys. Res. 89, 5215, 1984.
27. Green, A.E.S. and Xue, H., *Kinetic Modeling of Spectra of Flames with Suppressants*, International Journal of Quantum Chemistry, in press.
28. Green, A.E.S. and Pamidimukkala, K., *Kinetic Simulation of the Combustion of Gas/Coal and Coal/Water Mixtures*, Proc. 1st conf. on Combined Combustions of Coal and Gas, Cleveland, Ohio, 1982.
29. Green, A.E.S., Wagner, J., Saltiel, C. and Jackson, M., Proceedings of ASME Solid Waste Processing Conference, ASME, New York, 1992.
30. Wagner, J.C. and Green, A.E.S., *Correlation of Chlorinated Organic Compound Emission from Incineration with Chlorinated Organic Input*, Chemosphere, 26, No 11, 2039-2054, 1993.



31. Green, A.E.S., Vitali, J., and Miller, T., *Chlorobenzene Output from Combustion of Organic and Inorganic Compounds. Combustion Modeling Scaling and Air Toxins*, A.Gupta et al.Eds., ASME-FACT 18, 1-9,1994.
32. Green, A.E.S. and Pamidi, K.M., *Synergistic Combustion of Coal with Natural Gas*, Energy, Vol. 9, pp. 477-484, 1984.
33. Kee, R.J., Grcar, J.F., Smooke, M.D., Miller, J.A., *A Fortran Program for Modeling Steady Laminar One Dimensional Premixed Flames*, Sandia Report 85 8240 UC401, 1985.
34. Lewis, B.and von Elbe, g., *Combustion, Flames and Explosions of Gases*, Academic Press, New York, 1951.
35. Green, A.E.S., Schippnick, P.F., and URio, D.E., *Reactive Hydrogen- Oxygen Collisions in Combustion and Radiolysis*, Intern. Journ. Quant.Chem., 17, 127, 1983.
36. Cohen, N., *The Use of Transition-State Theory to Extrapolate Rate Coefficients for Reactions of OH, Oatoms and H Atoms with Alkanes*, Int. J. Chem. Kin.,14, 1339-1362, (1982); 18,99-140 (1986); and 23, 683-700, 1991.
37. Garrett, B.C. and Truhlar, D.G., *Reaction Rates for  $O + HD \rightarrow OH + D$  and  $O + HD \rightarrow OD + H$* , Int. J. Quantum Chem., 31, 17-31, 1987.
38. Urban, J. and Staemmler, V., *Theoretical Study of the Lowest Potential Energy Surfaces for the Reaction  $O + HBr \rightarrow OH + Br$*  Chem. Phys., 178, 279-286, 1993.
39. Bott, J.E. and Cohen, N., *A shock Tube Study of the Reactions of Hydroxyl Radical with Several Combustion Species*, Int. J. of Chem. Kin., 23, 1075-1094, 1991.
40. Truhlar D. G., and Garrett, B.C., *Resonance State Approach to Quantum Mechanical Variational Transition State Theory*, Jour. of Phy. Chem., 96, 6515. 1992.
41. Green, A.E.S., *Nuclear Physics*, McGraw Hill , New York, N.Y., 1955.
42. Leung, K.M., and Lindstedt, R.P., *Detailed Kinetic Modeling of C<sub>1</sub> - C<sub>3</sub> Alkane Diffusion Flames*, Combustion and Flame, 102, Elsevier Science Inc., July 1995.
43. Green, A.E.S. and Miller, J.H., *Atomic and Molecular Effects in the Physical Stage*, Physical Mechanisms in Radiation Biology, Atomic Energy Commission, 1974.
44. Mulholland, J.A., Sarofim, A.F., and Beer, J.M., *On the Derivation of Global Ignition Kinetics from a Detailed Mechanism for simple Hydrocarbon Oxidation*, Combust Sci. and Tech., 87, 139-156, 1992.
45. World Meteorological Organization, *Scientific Assessment of Ozone Depletion: 1944*, Global Ozone Research and Monitoring Project, Report No. 37.
46. Ewing, C.T., Faith, F.R., Hughes, J.T., and Carhart, H.W., *Evidence for Flame Extinguishment by Thermal Mechanisms*, Fire Technology, August 1989.
47. Morse, J.S. and Cundy, V.A., *Sooting in Chlorinated Hydrocarbon Combustion - A Critical Review*, Combustion Sci. and Tech., Vol 95, pp. 333-356, 1994.